[American Journal of Science, Vol. 305, April, 2005, P. 312–343]

AN EMPIRICALLY DERIVED KINETIC MODEL FOR ALBITIZATION OF DETRITAL PLAGIOCLASE

RENEE J. PEREZ*† and JAMES R. BOLES

University of California, Santa Barbara, Geological Sciences Department Room 1006, Webb Hall, Santa Barbara, California, 93106-9630

ABSTRACT. We propose an empirically derived model that estimates the extent of reaction for albitization of plagioclase as a function of time, grain surface area, and temperature from 0 to 200°C. We use a kinetic formulation independent of pressure, and consistent with the Rate Law, which quantifies the dependence of the reaction rate on the initial concentration of the reacting material, and the Arrhenius equation. The formulation is described by the function:

$$-\frac{d[An]}{dt} = S_m k[An_o]^2(1 - \bar{\Omega})$$

where $d[An]/dt$ is the rate change of the anorthite mole fraction with time, S_m the mineral surface area (cm^2), k the rate constant $1/cm^2$ s, $[An_o]$ is a constant representing the initial anorthite mole fraction, and $\bar{\Omega}$ a constant weighed average saturation index. We derive the apparent activation energy (E_a) and frequency factor (A), both present in the rate constant k, by fitting them to the extent of albitization measured in 11 samples from the San Joaquin Basin. Subsequently, we test the model against two independent albitization trends, one from the Texas Gulf Coast basin and one from the Denver Basin of Colorado. Our results indicate that albitization in all three basins can be fit by an E_a of 68 ± 4 kJ/mole and A of (6.5 ± 0.5) × 10^3 $1/cm^2$ Ma. The rate dependence on temperature is consistent with experimental values for albite crystal growth and with empirically derived precipitation rates of other diagenetic silicates such as illite and quartz. The parameters and fit suggest that albitization can be modeled as a surface controlled reaction, primarily dependent on temperature.

INTRODUCTION

Kinetics of Diagenetic Reactions

The aim of this paper is to present an empirical kinetic model for albitization of detrital plagioclase. The model is derived directly from geologic data and is applicable to at least three different sedimentary basins. Albitization, and most diagenetic reactions in general, are modeled empirically because (1) the extrapolation of laboratory measurements to geologic conditions generally requires very accurate and precise data that are so far not attainable, (2) small errors in the temperatures and heating rates during experimentation can become a major error in activation energies and orders of magnitude error in frequency factors (Burnham and others, 1987), and (3) changes in reaction mechanisms complicate the validation of kinetic parameters for wide temperature ranges (Comer, 1992). An alternative approach to estimate rate changes over large time scales (that is millions of years), is to model them using field observations and time-temperature burial data.

There are several examples of empirically derived reaction kinetics in geologic systems. Some, for instance, are the kinetics of petroleum generation (Lopatin, 1971; Waples, 1980), aromatization and isomerization of hydrocarbons (Mackenzie and Mackenzie, 1983; Gallagher and Evans, 1991), and vitrinite reflectance (Burnham and Sweeney, 1989). Similarly, empirically derived kinetics for illitization of smectite and

*Current affiliation: University of Calgary, Applied Geochemistry Group, Department of Geological Sciences, Calgary, Alberta T2N 1N4 Canada
†Corresponding author: Renee J. Perez, rene@earth.geo.ucalgary.ca

epitaxial quartz overgrowth receive special and continual attention due to their abundance in oil reservoirs (Walderhaug, 1994, 1996; Elliot and Mattissof, 1996). Our literature review reveals, however, that albitization of feldspar, although present in all rock settings, lacks a kinetic formulation useful for its prediction.

Albitization, A Brief Review

Albitization of plagioclase has been recognized since the turn of the twentieth century (for example, Bailey and Grabham, 1909). Perhaps the best reviews can still be found in Coombs (1954) and Deer and others (1963). In general, albitization refers to the transformation of any *An-Or-Ab* solid solution into albite. The solid solution is originally crystallized at high temperatures as igneous or metamorphic minerals, whereas the albite precipitates at low temperatures. Albitization results in low albite (Morad and others, 1990; Slaby, 1992), due to the high to low albite transition temperature of 575 ± 50°C (Smith, 1972; Moody and others, 1985). The newly formed albite is porous (Boles, 1982), which, as most replacement reactions, implies a dissolution/precipitation reaction mechanism such that the ion transport to the reaction interface and removal away from the interface are not diffusion-transfer limited (Putnis, 2002).

In sedimentary basins, albitization refers to a pseudomorphic replacement process that may imply a coupled dissolution of detrital plagioclase and precipitation of low albite at equal rates. The shape of the plagioclase parent crystal and internal structural details are preserved in the daughter albite crystal. *A priori*, coupled dissolution-precipitation reactions can not be considered to be controlled by the dissolution step (Luttge and Metz, 1991, 1993), however, isotopic analysis and kinetic experiments suggest that the major mechanism in feldspar replacement is dissolution followed by precipitation, and the rate-controlling step is grain surface dissolution (O'Neil and Taylor, 1967; Moody and others, 1985). Solid diffusion usually fails to explain albitization, mainly due to the presence of the peristerite or miscibility gap, which is evident in albitized grains by the presence of sharp reaction fronts separated by zones of constant composition (Fox, ms, 1989). Furthermore, isotopic analysis (O'Neil and Taylor, 1967; Stallard and Boles, 1989) and recent ^{18}O, H, D, and Na/(Na+K) mapping (Labotka and others, 2002) demonstrate that, during feldspar replacement, the oxygen isotope distribution re-equilibrates in the product, which indicates the breaking of Si-O and Al-O bonds, and the oxygen redistribution is facilitated by cation exchange (O'Neil and Taylor, 1967; Labotka and others, 2002). The preservation of internal details and oxygen re-equilibration strongly suggest that the replacement mechanism involves fine-scale solution and re-deposition in a structurally organized fluid film at the interface between the exchanged minerals (O'Neil, 1977; Putnis, 2002).

Albitization is probably one of the most common alumino-silicate reactions in the shallow crust of the Earth. It has been reported in deuterically altered granite and granodiorite (for example, Bailey and Grabham, 1909; Hess, 1950; Deer and others, 1963; Fox, ms, 1989), alkali-carbonatite complexes (Bodart, 1980), spilitized lava (Eskola and others, 1935; Rosenbauer and others, 1988), volcanic tuff (Coombs, 1954; Boles and Coombs, 1977), and sedimentary basins (Tester and Atwater, 1934; Middleton, 1972; Merino, 1975a; Land and Milliken, 1981; Boles, 1982; Gold, 1987; Boles and Ramseyer, 1988; Morad and others, 1990). Albitization is usually described with Al^{+3} conservative reactions that reproduce the characteristic volume conservation observed in thin sections. For example:

$$NaAlSi_3O_8 \cdot CaAl_2Si_2O_8 + H_4SiO_4 + Na^+ = 2NaAlSi_3O_8 + Al^{+3} + Ca^{+2} + 4OH^- \quad (1)$$

$$2SiO_2 + 0.5H_2O + H^+ + Na^+ + CaAl_2Si_2O_8 = NaAlSi_3O_8 + 0.5Al_2Si_2O_5(OH)_4 + Ca^{+2} \quad (2)$$

Merino (1975b) proposed equation (1), and Boles (1982) proposed equation (2). Reaction 2 assumes that silica is provided by quartz, instead of being supplied by pore fluid in the form of $Si(OH)_4$—for example $Si(OH)_4$ may be supplied from clay diagenetic reactions (Boles and Franks, 1979).

Importance

The question of which reaction best represents albitization, however, remains a subject of great debate but the implications are clear: overall consumption of Na^+, Si^{-4}, H^+, and release of Ca^{+2} and Al^{+3}. In other words, albitization reflects mass transfer (Merino, 1975b; Boles, 1982; Aagaard and others, 1990; Morad and others, 1990) and causes chemical changes in basinal pore fluids (Fisher and Boles, 1990; Davisson and Criss, 1996). Furthermore, albitization influences the porosity and permeability of fluid reservoirs, especially when CO_2 supply is constant. Kaolinite and calcite precipitation (as products of reactions 1 and 2) are commonly reported in the San Joaquin Basin as a consequence of the albitization of plagioclase (Merino, 1975b; Boles, 1984; Hayes and Boles, 1992; Wilson and others, 2000). Clearly, albitization is one of the most important and common reactions in all rock settings, and yet little is known about its transformation rate and predictability.

The Thermodynamic Problem

In spite of the reaction's universality, the temperature range of the so called "albitization zone" is not the same everywhere. Among some possible causes are the grain reactivity, degree of fracturing, initial composition, structural states (Ramseyer and others, 1992), and grain provenance (Boles and Ramseyer, 1988). Our literature review reveals, however, that the appearance of the albitization zone may be associated with differences in sediment ages and burial-thermal histories of the basins (Gold, 1987; Pittman, 1988; Ramseyer and others, 1992). This premise leads us to postulate that time, temperature, and heating rates may strongly influence the replacement zone as well, and that albitization is kinetically controlled by a critical activation energy.

One unanswered question is—Why are fluid compositions, at depths and temperatures less than the albitization zone, commonly in the *albite + dickite* stability field? (Merino, 1975b; Boles, 1982; Morad and others, 1990; Helgeson and others, 1993). Pore fluid compositions demonstrate that this is the case in several sedimentary basins (fig. 1). The equilibrium boundaries in figure 1 are based on reaction 2 assuming that the silica is provided by quartz. The estimated error on the equilibrium boundary, using errors assigned to the Gibbs free energy values at 25° C given by Robie and Waldbaum (1968), and using standard error estimate formulas is ± 1.0 pH unit (Boles, 1982). If silica is assumed to be provided by pore fluids, for example supplied by clay reactions (Boles and Franks, 1979) in the form of H_4SiO_4 in equilibration with quartz at the appropriate temperatures, the equilibrium boundaries would be 0.2 to 0.3 pH units higher at fixed calcium and sodium activity ratio ($\log([a_{Ca^{2+}}]/[a_{Na^+}])$) than those shown in the plot (Boles, 1982). If the aqueous silica concentrations were higher than required for equilibration with quartz, the albite-dickite stability field would expand even more, and pore fluid data would plot even further in the albite-dickite stability field. Additionally, reservoir fluids from the San Joaquin Basin are saturated with respect to albite, allowing low albite precipitation in open pore spaces at temperatures as low as 43°C, yet albitization (as a replacement) doesn't start until the temperatures are higher than 83°C (Boles and Ramseyer, 1988).

It is clear that fluid chemistry plays an important role in albitization (Baccar and others, 1993), but time and temperature may be the main controlling factors. In other

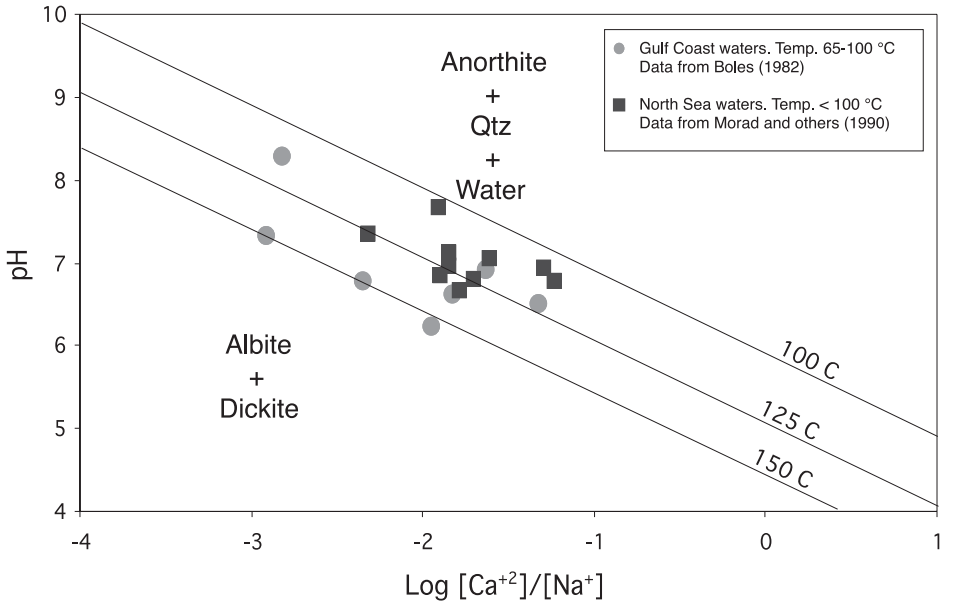

Fig. 1. Equilibrium boundary of albitization according to reaction 2 (see text), after Boles (1982). The error in the equilibrium constant calculated from free energy values given by Robie and Waldbaum (1968) is ~1 pH unit. We assume quartz provides silica. The plot shows that reservoir fluids are in the albite stability field and yet albitization was not observed.

words, the albitization zone is thermodynamically constrained by the pore fluid chemistry in basins. The reaction onset, however, is kinetically controlled and proceeds at an appreciable rate after a critical activation energy is reached, presumably at temperatures higher than 70°C.

RELEVANT KINETIC EXPERIMENTATION AND MODELING

There is a long tradition of dissolution and precipitation experiments and modeling involving feldspars; Helgeson and others (1984), Hellmann (1994), and Blum and Stillings (1995) give excellent reviews. Most experiments on albite precipitation have been performed at green schist and lower amphibolite *P-T-X* conditions (250-500°C and up to 1 kbar), generally in 0.1 M NaCl and 0.05 M Na_2SiO_3 solutions (Matthews, 1980; Moody and others, 1985). Alkali metal halides, such as NaCl and CaCl, have a dramatic effect on reaction kinetics (Winkler and Luttge, 1999), and it may be reasonable to consider that this is the case of subsurface environments. However, these temperature conditions are not observed in sedimentary basins and these experiments do not truly reproduce the nature of a pseudomorphic replacement (Merino and others, 1993).

Previous modeling of plagioclase albitization includes Baccar and others (1993) and Wilson and others (2000). The former study focused on the minimum time of albitization from 60 to 150° C in a closed system. It allowed a critical saturation before nucleation and growth, and assumed an initial fluid volume, fluid composition, and grain size distribution. The rate constants were derived using specific dissolution and precipitation kinetic constants and thermodynamic equilibrium constants. Baccar and others (1993) concluded that the albitization rate decreases with the extent of the reaction (which increases with temperature) and that plagioclase is not stable at high Pco_2 conditions. These results give insight into dissolution-precipitation processes,

such as the effect of Pco_2, but not into replacement mechanisms. The preservation of plagioclase internal details such as twin planes and cleavages, requires, among still many unknown parameters, at least: a) plagioclase to dissolve and albite to grow at equal and slow volumetric rates (Merino and others, 1993), b) a stress-controlled coupled dissolution/precipitation mechanism (Merino and Dewers, 1998), c) a structurally self-organized fluid film at the mineral interface (O'Neil and Taylor, 1967; Reyhani and others, 1999), and d) differences between parent and daughter crystal solubility (Putnis, 2002).

The latter study, (Wilson and others, 2000), considered albitization as a process independent of fluid composition. The model used an activation energy of 65 kJ/mol based on plagioclase dissolution experiments at low temperatures (Blum and Stillings, 1995) and fit the reaction order and the frequency factor to a single compositional data (Boles and Ramseyer, 1988). This empirical approach was useful to simulate the chemical evolution of the pore fluids in the San Joaquin Basin. It also proved to be successful by yielding results consistent with geologic observations. The model, however, lacked a chemical affinity term, validation in other settings, and was also independent of a surface area variable. After reviewing these two studies, we concluded that an albitization kinetic model could be better formulated by including a surface area variable, a saturation index term, and by testing it widely against data from several basins.

HYPOTHESIS

We postulate that the albitization rate is a function of time, temperature, fluid composition, and surface area. Our rate equation follows a kinetic formulation consistent with the Rate Law and the Arrhenius equation (Lasaga, 1984). Rate laws quantify the dependence of reaction rates on the concentration of the starting material. They take the general form:

$$\frac{dC}{dt} = kC^n \tag{3}$$

where dC/dt is proportional to the change in concentration of C raised to the power of n. The Arrhenius equation quantifies changes in the rate constant k with temperature and has the form:

$$k = Ae^{-E_a/Rt} \tag{4}$$

where A is the frequency factor, E_a the activation energy, R the universal gas constant, and T temperature. In our work, the kinetic parameters (E_a and A) present within the reaction rate k are fitted using solely molar compositional trends with depth, which are implicit functions of time and temperature. In reality, plagioclase composition, pore fluid pH, and temperature are the main controlling factors of the rate constant. However, different plagioclase compositions occur together in samples with identical pore fluid and temperature history, strongly suggesting that the chemical composition of the plagioclase has a stronger effect on the rate constant than pore fluid (Ramseyer and others, 1992). Furthermore, based on the following observations:

(1) pore water from marine basins have a limited initial variation in pH values and chemical composition (Fisher and Boles, 1990); and
(2) oil field brines are almost always in equilibrium or saturated with respect to albite and unsaturated with respect to anorthite (Helgeson and others, 1993),

We assumed that (1) albitization is a dissolution reaction, which should have an E_a between 40 and 80 kJ/mol (Lasaga, 1984), and (2) during albitization the sum of the anorthite, orthoclase, and albite mole fraction is one at all times.

The Saturation Index Hypothesis

The dissolution rate of a given plagioclase composition depends on the rate constant k, and the saturation index Ω. In our model the rate constant k is the fitted parameter and we will deal with it in more detail later. The saturation index Ω, at a fixed temperature and water composition, is commonly defined as:

$$\Omega = \frac{IAP}{K_{eq}} \tag{5}$$

where IAP is the ionic activity product of the solution, and K_{eq} the equilibrium constant. From the $\log_{10}\Omega$ positive numbers represent supersaturation and negative undersaturation (for example Bethke, 1996). Based on field observations that suggest that anorthite dissolution is the albitization rate-limiting step we assume that reaction 2 is adequate to represent albitization throughout geological time in sedimentary basins. Again, reaction 2 may be written as:

$$2\text{quartz} + 0.5\text{water} + H^+ + Na^+ + \text{anorthite} = \text{albite} + 0.5\text{dickite} + Ca^{+2} \tag{6}$$

in which the IAP is defined by:

$$IAP = \frac{a_{Ca} \cdot a_{dickite}^{1/2} \cdot a_{albite}}{a_{anorthite} \cdot a_{Na} \cdot a_H \cdot a_{H_2O}^{1/2} \cdot a_{quartz}^2} \tag{7}$$

where the a's are the activities of both, the solids and aqueous species. In this work, the solid phases were considered pure with unit activity, except anorthite. The anorthite content of plagioclase being albitized is ~0.35 mole fraction, and its activity is 0.45 (Saxena and Ribbe, 1972). The equilibrium constant K_{eq} is calculated from the Gibbs free energy of the reaction. The free energy change at any T and P and solution composition Q, in its simplest form, is given by:

$$\Delta_r G_{T,P} = \Delta_r H^\circ_{298} + \int_{298}^{T} \Delta_r Cp dt - T\left(\Delta_r S^\circ_{298} + \int_{298}^{T} \frac{\Delta_r Cp}{T}\, dt\right) + \int_{1}^{P} \Delta_r V dp + RT\ln Q \tag{8}$$

where $\Delta_r G_{T,P}$ is the Gibbs free energy $\Delta_r H^\circ_{298}$ enthalpy, $\Delta_r S^\circ_{298}$ entropy, $\Delta_r Cp$ heat capacity, and $\Delta_r V$ the molar volume change for the reaction, all in calories/mole (table 1). The subscript 298 refers to the reference temperature 298.15 Kelvin. At equilibrium, Q becomes K_{eq}, and the free energy change of the reaction is zero so that:

$$\ln K_{eq} = -\left[\Delta_r H^\circ_{298} + \int_{298}^{T} \Delta_r Cp dt - T\left(\Delta_r S^\circ_{298} + \int_{298}^{T} \frac{\Delta_r Cp}{T}\, dt\right) + \int_{1}^{P} \Delta_r V dp\right]/RT + \ln 0.45 \tag{9}$$

As shown above, the equilibrium constant for any reaction is ultimately a function of P, T, fluid composition, and solids composition. To calculate K_{eq} for reaction 2 we used thermodynamic data from two different, but consistent, sources. Free energies of formation, enthalpies of formation, and third law entropies for all solid phases were obtained from Robie and Waldbaum (1968). We used the database reported by Robie and Waldbaum (1968) instead of the more recent and standard database SUPCRT92 (Johnson and others, 1992) for the following reasons:

TABLE 1

Formation water compositions associated with partial or complete albitization. Data compiled from several sources

Reference	1	1	1	1	1	1	2	2	2	2	2	2	2	2
Well name	Swallow #4	Z.S. Ector	La Blanca	Kelley A-1	Gas Unit #15	JW Morin	78X-3	41x-10	58x-2	81x-3	24x-11	62x-11	66x-2	44x-2
Basin	TGCB	TGCB	TGCB	TGCB	TGCB	TGCB	SJB	SJB	SJB	SJB	SJB	SJB	SJB	SJB
Formation	Frio	Frio	Frio	Frio	Frio	Frio	Stevens	Stevens	Stevens	Stevens	Stevens	Stevens	Stevens	Stevens
Field	Dona	North Cano	La Blanca	Pharr	Welasco	Donna	Paloma	Paloma	Paloma	Paloma	Paloma	Paloma	Paloma	Paloma
Depth	2395.0	2672.0	2903.0	3018.0	3086-3118	3170.0	3607.0	3583.0	3632.0	3705.0	3686.0	3708.0	3772.0	3775.0
Temp. C	110.0	110.0	148.0	127.0	125.0	135.0	119.0	119.0	120.0	122.0	114.0	132.0	160.0	134.0
Na	5711.0	4627.0	2680.0	9420.0	3191.0	6725.0	7029.0	6841.0	7776.0	7285.0	5610.0	4725.0	5305.0	4383.0
K	ND	197.0	46.0	240.0	NI	NI	129.0	194.0	157.0	133.0	185.0	129.0	118.0	147.0
Mg	36.0	44.0	3.3	18.0	20.0	30.0	1.1	4.8	7.1	2.3	0.5	0.3	6.7	0.3
Ca	2128.0	992.0	150.0	4225.0	800.0	110.0	5696.0	1806.0	1740.0	5376.0	3239.0	4253.0	6905.0	8724.0
Sr	NI	NI	9.6	256.0	NI	NI	100.0	70.0	97.0	95.0	106.0	102.0	161.0	180.0
Ba	NI	NI	1.5	27.0	NI	NI	6.6	3.2	4.9	5.5	4.5	7.5	4.4	1.6
Cl	12375.0	8830.0	3950.0	22000.0	5780.0	9865.0	17025.0	13507.0	14036.0	17490.0	13612.0	15108.0	20038.0	20639.0
Br	NI	NI	15.0	78.0	NI	NI	96.0	78.0	95.0	184.0	48.0	89.0	96.0	100.0
I	NI	NI	16.0	22.0	NI	NI	0.5	0.7	0.4	0.6	11.5	50.9	19.6	93.3
B	NI	NI	117.0	105.0	NI	NI	52.5	42.8	42.2	56.8	44.2	50.4	23.2	60.1
NH3	NI	NI	4.2	21.5	NI	NI	NI	NI	NI	NI	NI	NI	NI	NI
HCO3	293.0	332.0	400.0	114.0	527.0	1129.0	NI	557.0	565.0	716.0	530.0	2645.0	1026.0	1038.0
SO4	175.0	410.0	57.0	7.0	420.0	175.0	NI	NI	NI	NI	NI	NI	NI	NI
*SiO3	NI	NI	88.0	90.0	NI	NI	NI	52.4	70.2	51.5	51.4	49.4	36.6	49.0
pH	6.3	7.2	7.3	6.8	7.3	6.4	7.2	7.1	6.8	6.9	6.7	7.2	7.0	6.9
TDS	20968.0	15432.0	7500.0	36600.0	10738.0	18250.0	NI	NI	NI	NI	23344.0	27110.0	33775.0	35233.0

Concentrations in mg/liter
*Reported as Si
TGCB = Gulf Coast Basin
SJB = San Joaquin Basin
NI = No Information
References 1) Boles (1982); 2) Fisher and Boles (1990).
Temperature in degrees Celsius
Depth in meters

a) Consistency with previous studies. Boles (1982) determined the albitization stability field and errors in the free energy of formation and equilibrium constant of reaction 2 using the Robie and Waldbaum (1968) database.
b) Contrary to Robie and Waldbaum's database, SUPCRT92 lacks standard enthalpy and Gibbs free energy data for Dickite, which is part of the products in the reaction under study.
d) Robie and Waldbaum's database contains thermodynamic data for Dmisteinbergite, an hexagonal anorthite polymorph used, as we will explain later, as a proxy to evaluate the influence of the atomic arrangement and crystalline structure on the transformation kinetics.

On the other hand, the standard Gibbs free energy, enthalpy and entropy of formation of anorthite, low albite, and quartz present in Robie and Waldbaum (1968) differ by less than 1.4 percent from those present in SUPCRT92, so, in spite of the other differences, we felt comfortable using heat capacity data from SUPCRT92 as summarized by Anderson and Crear (1993).

In order to keep our model simple and ease the calculation of the equilibrium constant we made several simplifications. First, justified by the narrow range of temperatures being considered here, we assumed that the heat capacity for ions was constant. We also assumed that our model is pressure independent, and the *net* solid volume change is close to zero (Boles, 1982) thereby assuming $P = 1$ bar in equation (9) and neglecting the pressure correction term. Consequently, $\ln K_{eq}$ is left as a function of temperature and can be represented by the following polynomial equation:

$$\log_{10} K_{eq} = p_1 T^3 + p_2 T^2 + p_3 T + p_4 \tag{10}$$

where $p_1 = -1.7513 \times 10^{-7}$, $p_2 = 2.7925 \times 10^{-4}$, $p_3 = -0.1685$, and $p_4 = 37.993$ (fig. 2). The error in the equilibrium constant at 298.15 K, calculated from standard error estimation formulas is $\pm$ 0.98. It is likely that this error may expand at higher temperatures. The thermodynamic values used are summarized in table 2. As we will discuss further in the text, we plan to qualitatively examine the effect of the anorthite crystalline structure on albitization, in other words, on reaction 2. Thus, figure 2 also illustrates the $\log_{10} K_{eq}$ for reaction 2 assuming that an hexagonal anorthite (an anorthite polymorph) detrital grain is being albitized, in which case we use different standard free energy and entropy values (table 2). Heat capacity data for hexagonal anorthite are, to our knowledge, not available, so we retained the same heat capacity equations. The equilibrium constant for reaction 2 assuming hexagonal anorthite can also be fitted to equation (10) with different coefficients: $p_1 = -1.4412 \times 10^{-7}$, $p_2 = 2.2995 \times 10^{-4}$, $p_3 = -0.13938$, and $p_4 = 30.421$. The error in $\log_{10} K_{eq}$ is larger than $\pm$ 0.98, but no further calculations were performed.

Speciation and ion activities were, on the other hand, calculated with SOLMINEQ.88 (Kharaka and Barnes, 1973; Perkins and others, 1990). We used reservoir fluid compositions from the San Joaquin and Gulf Coast Basins, at depth intervals where albitization is present and thermodynamically active (see our table 1; data from Boles, 1982; Fisher and Boles, 1990). Based on the water chemistry data we assumed that the oil field waters are in equilibrium with quartz, so that the activity of the solid quartz activity is one. This assumption is justified by the presence of authigenic quartz in intervals above the albitization zone, also by fluid chemistry data (Wilson and others, 2000). The SOLMINEQ.88 code is only partially consistent with the origins of the thermodynamic database presented in table 2. However, the analyzed Na^+ and Ca^{+2} concentrations in the reservoir waters differ by less than 10 percent from those concentrations calculated by the code, clearly indicating that the

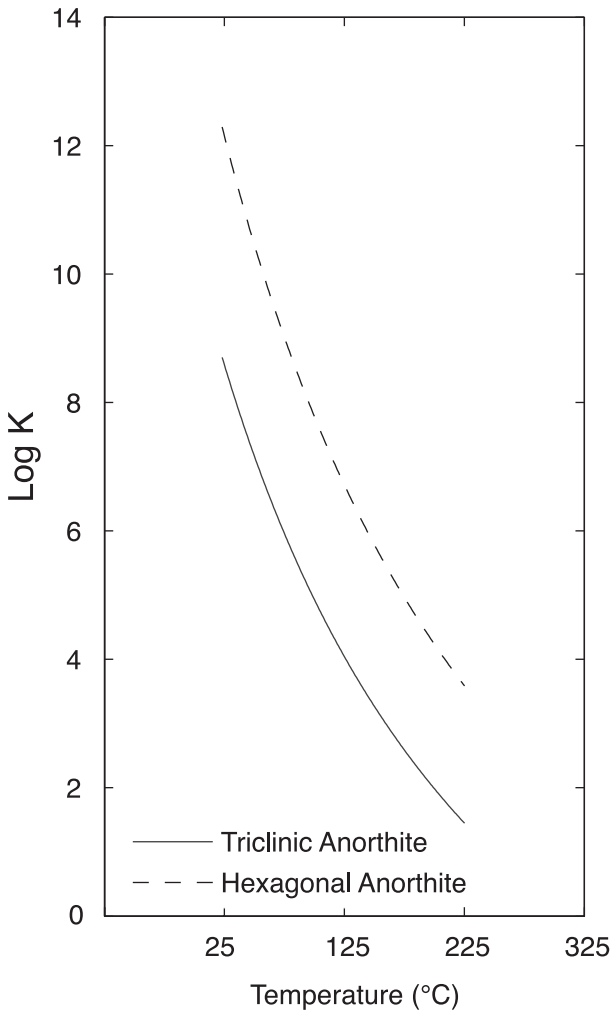

Fig. 2. Plot showing the equilibrium constant for reaction 2 assuming pure anorthite and its hexagonal polymorph (see text). The $\log_{10}K$ is calculated with equation (9) as a function of temperature. Thermodynamic data is from Robie and Waldbaum (1968) and Johnson and others (1992). The error in $\log_{10}K$ (anorthite) at 298.15 K and 1 bar, calculated from standard error estimation formulas and from thermochemical errors in the former database is $\pm$ 0.98. It is likely that this error may expand at higher temperatures.

complexation of these ions in minerals is negligible. Consequently, any thermodynamic calculation of Na^+ and Ca^{+2} activities would be consistent with the thermodynamic database used in our paper. The resulting activities, ionic activity products, and equilibrium constants for a variety of fluid compositions and temperatures used in our model are shown in table 3.

The former table shows the variation of the saturation index from San Joaquin and Gulf Coast Basin fluids that are currently at temperatures between 100 and 130° C, and where albitization is actively occurring (Boles, 1982). However, considering the waters' ages are considerably different, in general several millions of years of difference, and that they have gone through different time-temperature paths, it could be considered that the variation of Ω is relatively small. Thus, given 1) the narrow range of

TABLE 2

Thermodynamic values used to calculate the equilibrium constant for reaction 2

Phases	*Stoichiometry*	$\Delta G°(298,1)$	$\Delta H°(298,1)$	$S°(298,1)$	*Heat Capacity (298)* a	$bx10^3$	$cx10^{-5}$
SiO_2	2	-204646	-217650	9.88	11.22	8.2	-2.7
H_2O (l)	0.5	-56688	-68315	16.71	12.665	0	0
$H^+_{(aq)}$	1	0	0	0	0	0	0
$Na^{+(aq)}$	1	-62591	-57433	13.96	4.95	0	0
Anorthite	1	-955626	-1009300	48.45	63.311	14.794	-15.44
**Hexagonal Anorthite*	1	-949958	-1004410	45.84	63.311	14.794	-15.44
Low Albite	1	-883988	-937146	50.2	61.7	13.90	-15.01
Dickite	0.5	-902142	-979165	47.1	72.77	29.20	-21.52
$Ca^{+2(aq)}$	1	-132180	-129800	-13.5	11.089	0	0
	∑ *Reactants*	-1455853	-1536190.5	90.53	103.831	31.194	-20.847
	∑ *Products*	-1467179	-1556528.5	60.25	90.555	28.50	-25.77
	* ∑ *Products*-∑ *Reactants*=	-11326	-20338	-30.28	-13.276	-2.694	-4.923
	∑ *Reactants*	-1450185	-15231300.5	87.92	103.831	31.194	-20.845
	∑ *Products*	-1467179	-1556528.5	60.25	90.555	28.50	-25.77
	** ∑ *Products*-∑ *Reactants*=	-16994	-25228	-27.67	-13.276	-2.694	-4.93

*Delta of the reaction assuming anorthite
**Delta of the reaction assuming hexagonal anorthite
$\Delta G°$ = Standard Gibbs Free Energy of Formation (Calories/mole)
$S°$ = Standard Entropy "Third Law" of phase (Calories/K mole)
$\Delta H°$ = Standard Enthalpy of Formation (Calories/mole)
a = Calories/mole
b = Calories/mole K^2
c = Calories/mole K^5
The sum considers the stoichiometry of the reaction
Heat capacity of pure phases and thermodynamic data for aqueous ions from SUPCRT92 and summarized by Anderson and Crear (1993)

compositions of albitized detrital plagioclase grains, 2) the relatively small Ω variations for waters of considerably different ages (millions of years) and different *T-t* paths, and 3) the occurrence of different plagioclase compositions in samples with identical pore fluid and temperature history, we hypothesize that a weighted average integration of a saturation index as a function of temperature, may be useful to simplify the variations of water chemistry of the studied basins.

All our assumptions may seem, a priori, very simplistic and far from realistic but they are constrained by field data and petrographic observations, and they are not unreasonable. First, normally all replacement reactions are considered isovolumetric (Merino and others, 1993; Nahon and Merino, 1997; Merino and Dewers, 1998). Second, it might be justified that during the pseudomorphic replacement, the coupled dissolution-precipitation of plagioclase and albite, establishes locally a small-scale steady state or at least a "quasi" steady state composition of the pore fluid, leading to a local saturation that could be assumed to be about constant over long time intervals. This idea would be particularly justified if the Al^{+3} and Ca^{+2} leave the local system at a constant rate and fluid transport would not be too fast, as in the case in deep crustal settings away from fractures and faults, where permeabilities could be in the range of tenths of milidarcies and the average flow velocity is, at times, less than 1 cm/Ma (Garven, 1995).

TABLE 3

Input data for saturation index calculation. Speciation performed with SOLMINEQ.88

Sample ID	***Activities***					***Anorthite***			***Hexagonal Anorthite***		
Well	***[Na]***	***[Ca]***	***[H]***	***[H_2O]***	***IAP***	***K_{eq}***	***IAP/K_{eq}***	***LOG(IAP/K_{eq})***	***K_{eq}***	***IAP/K_{eq}***	***LOG(IAP/K_{eq})***
Gas Unit #15	0.0997	0.00623	5.012E-08	0.9943	2778501.225	13148.25212	211.3209573	2.324942569	191.8764062	14480.68202	4.160789017
JW Morin	0.203	0.0007649	3.981E-07	0.9898	21141.22785	6784.237307	3.116227646	0.493629176	109.7887961	192.5627078	2.284572184
Swallow #4	0.1687	0.01436	5.012E-07	0.9888	379543.4949	37715.65198	10.06328871	1.002739933	466.2988342	813.9490538	2.910597223
ZS Ector	0.1322	0.005781	1.622E-07	0.9919	601553.4272	37715.65198	15.94970246	1.202752586	466.2988342	1290.0599	3.110609876
La Blanca #12	0.08176	0.0009879	0.0000002	0.9957	134544.3112	3000.16858	44.84558371	1.651719681	55.10833956	2441.451008	3.387648014
Kelley A-1	0.2467	0.01928	5.537E-07	0.9804	316773.7541	11489.66044	27.5703321	1.440441997	171.2504188	1849.769223	3.267117549
78x-3	0.1864	0.02716	5.528E-07	0.9842	590420.7731	19858.53935	29.73132931	1.473214327	271.6400041	2173.54132	3.337167901
41X-10	0.1869	0.009181	2.404E-07	0.9875	456946.2912	19858.53935	23.0100655	1.361917855	271.6400041	1682.175984	3.225871428
58X-2	0.211	0.008517	3.373E-07	0.9866	267734.7736	18524.25682	14.45319919	1.159963988	256.1738215	1045.129327	3.019170034
81x-3	0.1921	0.02436	3.771E-07	0.9838	753403.2058	16134.77387	46.69437649	1.669264581	228.0214618	3304.08901	3.519051738
24x-11	0.1534	0.01657	4.436E-07	0.9878	544450.7328	28261.64319	19.26465241	1.284761178	365.6940806	1488.814727	3.172840656
62x-11	0.1236	0.01712	2.178E-07	0.987	1422513.262	8247.119062	172.4860829	2.23675406	129.4597059	10988.07735	4.040921708
66x-2	0.1308	0.02538	0.000000344	0.9835	1263937.896	1470.603283	859.4689747	2.934230204	30.15119629	41919.99163	4.622421187
44x-2	0.1122	0.03572	3.721E-07	0.983	1917651.35	7238.308408	264.9308709	2.423132567	115.9601503	16537.1582	4.218460881

IAP Ionic activity product Keq Equilibrium constant

GENERAL KINETIC MODELS AND EQUATIONS

Lasaga (1984, 1995, and 1998) explains all theoretical and fundamental approaches to describe dissolution and precipitation rates of minerals. The general kinetic formulation for mineral/fluids interactions is equation (11):

$$Rate = S_m(Ae^{-E_a/RT})a^n_{OH^-} \cdot g(I) \prod_i a^{n_i}_i f(\Delta_r G) \tag{11}$$

where the *Rate* is a function of the reactive surface area S_m (cm^2), the frequency factor A (1/s), the apparent overall activation energy E_a (kJ/mol) the temperature T (K), the universal gas constant R (J/K mol), the OH^- activity raised to the power of n $a^n_{OH^-}$ (dimensionless), the ionic strength of the solution $g(I)$ (I has units of molality times the ionic charge squared), the activity products a^n_i of the rate-determining specie i (dimensionless) raised to the power of n, and a general function of the free energy of the reaction $f(\Delta_r G)$ that can take many forms, where $\Delta_r G$ has units of J/mol. Another widely used empirical kinetic model, written as an adaptation of equation (11) by Aagaard and Helgeson (1982) is:

$$Rate = S_m k_m a^m_i (1 - \Omega) \tag{12}$$

where S_m is the interfacial area (cm^2) between the mineral and the aqueous solution, k_m is the rate constant (1/s), a^n_i is the activity of the rate-determining aqueous species i in solution. On the other hand, the kinetics of pseudomorphic replacement have been formulated with two simultaneous reactions that occur at equal volumetric rates, driven by a force of crystallization generated by supersaturation (Maliva and Seiver, 1988; Dewers and Ortoleva, 1990; Merino and others, 1993; Nahon and Merino, 1997). In this case, the sum of the rates equals zero as in equation (13)

$$R_a + R_b = 0 \tag{13}$$

where R_i is the linear dissolution rate of mineral i in cm/s represented by equation (14):

$$R_i = k_i(1 - \Omega) \tag{14}$$

where k_i (cm/s) and Ω_i have the usual meanings. Equations (11) through (14) depend on the aqueous ionic species present during the reaction and are founded on a well-developed physical-chemical theoretical basis, and only laboratory-based measurements, with good control of fluid composition (in either closed or open systems) can be most easily used for a rigorous interpretation of kinetic rate laws and reaction mechanisms. However, the prediction and modeling of the fluid saturation path in sedimentary basins is far from attainable. The variation and evolution of chemical and ionic species through geologic time is even more difficult to predict or model with precision. Furthermore, invalid extrapolations of experimental kinetic parameters to geological settings and our poor understanding of reaction mechanisms (and of many other variables) limit the applicability of rigorous and experimental approaches to field examples.

Based on the reasons explained previously, most empirical models of diagenetic reactions take a different and simple approach; they reduce and ignore a vast amount of variables, specifically fluid compositions by avoiding or leaving constant the saturation index or chemical affinity parameter in the rate expression. The models lack a physical-chemical basis (Oelkers and others, 2000), however, they can successfully predict dissolution and precipitation over long time scales, which is the ultimate goal of these studies.

The smectite to illite conversion during shale diagenesis provides one example of empirically derived kinetics. Several models for this particular reaction have been proposed and evaluated (Elliot and Matisoff, 1996). The most recent model (Huang and others, 1993) computes the rate with:

$$-\frac{dS}{dt} = k[\mathrm{K}^+]S^2 \tag{15}$$

where dS/dt is the change of the smectite fraction with respect to time t, k is the rate constant, $[\mathrm{K}^+]$ is a fixed and constant potassium concentration (in ppm), and S is the dimensionless fraction of smectite in the illite/smectite raised to the power of 2.

Another example is quartz overgrowth precipitation. Commonly, models for quartz precipitation couple diffusion, kinetic, and thermodynamic aspects of the reaction (Oelkers, 1996; Oelkers and others, 2000). In contrast, a simpler mathematic/kinetic model based on time-temperature and surface area (Walderhaug, 1994 and 1996) continues to be successfully tested in basins around the world (for example Awwiller and Summa, 1997; Lander and Walderhaug, 1999; Perez and others, 1999a, 1999b). The quartz precipitation model uses a logarithmic rate function dependent on temperature (eq 16):

$$Rate = a10^{b\cdot T(t)} \tag{16}$$

where a (moles/cm^2) and b (1/°C) are pre-exponential and exponential constants and $T(t)$ is temperature expressed as a function of time. The precipitated quartz volume Vq (cm^3) is calculated as a sum of integrals within sequences of time steps i (eq 17):

$$Vq = \frac{M}{\rho}\, a \sum_{i=1}^{n} \left(A_i \int_{t_i}^{t_{i+1}} 10^{b\cdot T(t)} dt \right) \tag{17}$$

where M is quartz molar volume (g/mole), ρ is quartz density (g/cm^3), A_i is surface area (cm^2), and t is time (sec). As we explained previously, these empirical models depend mainly on the variations of the heating rate through geologic time, obtained through basin modeling (Siever, 1983), and lack an affinity term.

ALBITIZATION KINETIC MODEL

Based on previous formulations in the San Joaquin Basin (Wilson and others, 2000), we modeled albitization with a kinetic/mathematical formulation expressed in equation (18) by:

$$-\frac{d[An]}{dt} = S_m k[An_o]^2(1 - \bar{\Omega}) \tag{18}$$

where $d[An]/dt$ is the change of the anorthite mole fraction with respect to time t, k is the rate constant in 1/cm^2 s, $[An_o]^2$ is the initial anorthite mole fraction squared, and $\bar{\Omega}$ the weighted average saturation index. In equation (18) S_m is the area of the mineral-solution interface (Lasaga, 1984) and is expressed in equation (19) in the following form:

$$S_m = \frac{A_m}{V_m} \cdot v \tag{19}$$

where, A_m is the mineral surface area (cm^2), V_m is the mineral volume assuming spherically-shaped grains (cm^3), and v is the unit volume of the sandstone, which

includes porosity and is equal to 1 cm^3. Simplifying, the surface area interface results in equation (20):

$$S_m = \frac{6}{d} v \tag{20}$$

where d is the grain diameter (cm). In all analyzed samples the grain size ranges from 0.012 ± 0.001 to 0.086 ± 0.018 cm, varying from one sample to another, however, average grain diameter is 0.031 ± 0.002 cm (table 4). These values are obtained by measuring the mean grain diameter in 40 grains per thin section, using a standard polarized light petrographic microscope.

The rate constant k follows the Arrhenius equation (21):

$$k = A \exp\left[\frac{-E_a}{RT(t)}\right] \tag{21}$$

where A and E_a are apparent pre-exponential and exponential parameters in $1/cm^2$ s and kJ/mole respectively, R the universal gas constant (J/K mole), and $T(t)$ is temperature in K expressed as a function of time t.

The initial anorthite molar fraction value $[An_o]$ is obtained through field measurements. It is determined on detrital plagioclase grains with an ARL microprobe analyzer, model SMX-SM equipped with three wavelength-dispersive spectrometers and a Tracor Northern TN2000 energy dispersive system, by simultaneously analyzing for sodium, potassium, and calcium, aluminum, and silicon. Each grain is analyzed *on* the rim and *in* the core, and 50 grains are usually analyzed per thin section from different depth intervals and temperatures (Boles, 1982; Boles and Ramseyer, 1988; Pitmman, 1988).

Based on the reasons explained above we used a mean saturation index term $\bar{\Omega}$ ($\bar{\Omega} \neq \Omega$) obtained with a weighted average integration. The method to obtain $\bar{\Omega}$ is as follows: a) first we calculate several numerical values of Ω (defined in equation 5) using waters compositions from different reservoirs of different ages, depths and burial temperatures where albitization is active (table 3); b) observing a slight temperature dependence of these values, we fit them to a function of temperature–which is implicitly a function of time; c) we weight averaged the function with equation (22), so that:

$$\bar{\Omega} = \frac{\int_T \Omega(T)\,dT}{\int dT} \tag{22}$$

The integration along the $\Omega(T)$ function (solution to equation 22), neglecting the extreme values and within the temperature of interest, results in a constant $\log_{10}\bar{\Omega} = 2.632$. This positive number suggests that pore fluid compositions are in the albite + dickite stability field, which is consistent with field observations. In short, to start the albitization, pore fluids must be supersaturated with respect to albite, that is, in the albite stability field according to reaction 2.

It is well known that, in laboratory experiments, dissolution and precipitation reactions are usually not independent of fluid composition, and such assumption would only be valid if the reaction occurs far from equilibrium. Thus, a constant $\bar{\Omega}$ may be somewhat problematic. However, based on (1) the small range of water composi-

TABLE 4

Summary of data sets used as input in our model. Data include unpublished well names, and samples' temperature, age, and grain size.

						Average Composition in molar %							
Basin	*County/Field*	*Well name*	***Depth (m)*	****Temp.(in C)*	*Age (Ma)*	*Ab*	*s.d.*	*Or*	*s.d.*	*An*	*s.d.*	*Grain size*	*s.d.*
Gulf Coast													
1	Jim Wells	Humble Tarrant	1109.0	52.5	28.5	60.3	N.I.	4.6	N.I.	35.1	8.6	0.16	0.04
2	Hidalgo	Bryan Hanks	2519.0	96.3	31.50	74.3	N.I.	3.5	N.I.	22.0	18.2	0.15	0.04
3	Hidalgo	S.Welasco	3104.0	122	29	96.7	N.I.	1.5	N.I.	1.8	0.9	0.19	0.03
4	Willacy	Willamar	3878.0	128	30.2	97.3	N.I.	0.6	N.I.	2.1	5.5	0.11	0.01
5	Kenedy	S.K.East 41	4005.0	136	30.8	99.0	N.I.	0.5	N.I.	0.5	0.2	0.13	0.01
6	Kenedy	S.K.East B20	4329.0	141	32	98.3	N.I.	0.7	N.I.	1.0	1.1	0.13	0.02
7	Kenedy	John Kennedy J-3	4394.0	145	33	99.0	N.I.	0.4	N.I.	0.6	0.5	0.17	3
8	Kenedy	Risken #2	4409.0	145	33	99.1	N.I.	0.4	N.I.	0.5	0.4	0.12	0.01
San Joaquin Basin													
1	Strand	Ohio KCL 86-1	2841.7-2488.3	90	6.7	68.9	8.7	1.2	0.6	29.8	8.8	0.28	0.04
2	Wildcat	Ohio KCL G-1	3211.9-3212.5	104	8.5	68.1	7.6	1.8	0.8	30.1	7.4	0.35	0.03
3	South Coles Levee	KCLB 67-4	2925.0-2927.4	113	10.2	71.9	10.3	1.1	1.8	27.4	13.2	0.62	0.03
4	Paloma	74-2	3353.1-3363.1	122	13.6	76.8	9.9	1	0.6	22.6	9.9	0.23	0.03
5	Wildcat	Teneco 26-29	4253.4	156	25.2	94.8	5.3	0.9	0.7	4.4	5.2	0.65	0.24
6	Wildcat	T.S.Hills 64X-34	5581.4	159	25.2	97.5	2.5	0.3	0.6	2.2	2.3	0.86	0.18
7	Paloma	KCL A72-4	4420.7	160	25.2	93.4	8.1	0.5	0.8	6.1	7.7	0.25	0.03
8	Paloma	KCL A72-4	4614.3	167	29.5	96.5	5	0.8	0.5	2.8	4.8	0.81	0.27
9	Paloma	KCL A72-4	4682.0	169	33.7	96.6	4	0.6	0.7	2.9	3.7	0.51	0.13
10	North Coles Levee	CLA 67-29	4808.5-4816.5	174	33.6	96.5	5	0.5	0.4	3.1	4.8	0.07	N.I.
11	Wildcat	T.S.Hills 64X-34	6204.0	175	35.1	96.1	2.5	0.2	0.5	3.7	2.3	0.75	0.18
Denver Basin													
1	Spindle	Rademacher No.1	1283.2**	58.9	73.3	N.I	N.I	N.I	N.I	10.5	12.4	0.088	N.I.
2	Spindle	Rademacher No.1	1286.9**	58.9	73.3	N.I	N.I	N.I	N.I	12.3	13.3	0.177	N.I.

*Gulf Coast Basin data from Boles (1982), the San Joaquin Basin data from Boles and Ramseyer (1988) and the Denver Basin data from Pittman (1988)
**Present day depth
***Present day temperature
Ab stands for ablite, *Or* for orthoclase and *An* for anorthite
s.d. stands for standard deviation of spot analysis per sample [100 spots for Boles (1982) and Boles and Ramseyer (1988) and 20–27 spots for Pitmann (1988)]
N.I. No information
The grain size units are in millimeters

tions present in the San Jaoquin and Gulf Coast Basin where albitization is active (Boles, 1982), (2) a narrow albitization temperature window, (3) the relatively small range of albitized plagioclase compositions (fig. 2), we propose that the heating rate may be the most important parameter for the actual kinetics of the replacement. Particularly because experiments suggest that this is the case when the reaction products grow *on* the reactant (Luttge and others, 1998), as in the case of replacement reactions.

In addition, at depths greater than 3 to 4 km, where albitization occurs, the rock permeabilities are on the order of the tenths of milidarcies and the rate of fluid transport is very small; and it is reasonable to assume that some minerals can establish locally a steady state or at least a "quasi" steady state composition of the pore fluid, leading to a local saturation that could be assumed to be about constant over long time intervals.

Numerical Solution

The solution of equation (18) is reached by the integration of equation (23):

$$\int d[An] = -\int_{t_0}^{t_m} Ae^{-E_a/R\cdot T(t)} \frac{6}{d} v[An_o]^2(1-\bar{\Omega})dt \tag{23}$$

An analytical integration of the right hand side of equation (23) from time t_0 to t_m is not trivial due to the time dependence of the temperature, and some proposed rational approximations (for example Burnham and others, 1987) introduce errors at high temperatures (Comer, 1992). Alternatively, a numerical solution can be reached if $\bar{T}(t)$ is divided in increments, and a mean value $\langle \bar{T} \rangle_i$ is calculated within the $(i) - (i+1)$ time steps. In the general case, the mean temperature $\langle \bar{T} \rangle_i$ may be calculated through a weighted average integration expressed in equation (24) as:

$$\langle \bar{T} \rangle_i = \frac{\int_{t_i}^{t_{i+1}} T(t)dt}{\int_{t_i}^{t_{i+1}} dt} \tag{24}$$

If the increments are small and considered linear, $T(t)$ takes the form of equation (25)

$$T(t) = \sum_{i=1}^{n} m_i t + d_i \tag{25}$$

where the slope m is the temperature change rate (in °C/s), t is time, and d is the initial temperature (in °C), and $\langle \bar{T} \rangle_i$ is reduced to an average between two time steps, that is $(T_i + T_{i+1})/2$. If a time-temperature curve, represented by the function $T=T(t)$, is divided in small linear increments from (T_i, t_i) to (T_{i+1}, t_{i+1}), the slope m_i between each interval would be:

$$m_i = \frac{T_{i+1} - T_i}{t_{i+1} - t_i} \tag{26}$$

and the initial temperature d_i is:

$$d_i = T_i - \left(\frac{T_{i+1} - T_i}{t_{i+1} - t_i}\right) t_{i+1} \tag{27}$$

Our model uses variable times steps, between 0.3 and 0.7 million years, depending upon the sample age and temperature history. The model results are independent of the time step length, although intervals of 0.5 million years are preferred because they give best results. The substitution of $T(t)$ by $\langle \bar{T} \rangle_i$ results in equation (28):

$$\int d[An] = -\int_{t_i}^{t_{i+1}} Ae^{-E_a/R\cdot\langle \bar{T} \rangle} \frac{6}{d} v[An_o]^2(1 - \bar{\Omega})dt \tag{28}$$

Although equations (23) and (28) may seem similar, the substitution simplifies the integration, because $\langle \bar{T} \rangle$ is now a constant. Finally, the integration is numerically expressed with equation (29):

$$[An]_{i+1} = \sum_{i=0}^{n} \left([An_o]_i - \mathrm{Ae}^{-E_a/R\langle \bar{T} \rangle_i} \frac{6}{d} v[An_o]_i^2(1 - \bar{\Omega})(t_{i+1} - t_i) \right) \tag{29}$$

where i is the time step.* During albitization of detrital plagioclase in the studied basins, the anorthite mole fraction decreases from $\sim An_{35}$ to An_0, and the albite mole fraction increases simultaneously from Ab_{65} to Ab_{99} (table 4). By definition the sum of the mole fractions is unity, that is:

$$An + Ab + Or = 1 \tag{30}$$

where *An, Ab,* and *Or* are the anorthite, albite, and orthoclase mole fractions. Therefore, the simultaneous gain of the albite component, as a result of albitization, is computed with equation (31)

$$[Ab]_{i+1} = 1 - \sum_{i=1}^{n} \left([An_o]_i - Ae^{-E_a/R\langle \bar{T} \rangle_i} \frac{6}{d} v[An_o]_i^2(1 - \bar{\Omega})(t_{i+1} - t_i) \right) - [Or_o] \tag{31}$$

where $[Ab]$ is the final albite mole fraction per time step i, $[Or_o]$ is the initial orthoclase mole fraction that could be set constant to 0.05 ± 0.01, or simply ignored.

The only unknown parameters in equation 29 are E_a and A. When only two parameters are being optimized, both least squares fit and direct search techniques are efficient methods (Gallagher and Evans, 1991). We approached the problem with a direct grid search, using an iteration method, which breaks the time-temperature domain into a series of discrete blocks, where equations 23 through 31 are calculated. We began our search of A by fixing E_a from 60 to 70 kJ/mol following Walther and Wood (1984) and Lasaga (1984). We decided to search with small E_a and wide A increments. Our decision was based on the limited E_a range ($60 > E_a < 80$ kJ/mol) reported for a great number of dissolution reactions of alumino silicates (Lasaga, 1984) and specifically for feldspar hydrolysis reactions at neutral pH within the temperature of interest (Hellman, 1994; Blum and Stillings, 1995).

As input, we used (1) compositional data that revealed increasing albitization with depth and temperature (table 2), and (2) time-temperature curves obtained through 1-D burial-thermal modeling of the basins. We performed the basin modeling using Genesis^{tm} (Zhiyong, 2003).

*Note that $[An_o]_i^2$ is a constant per time step.

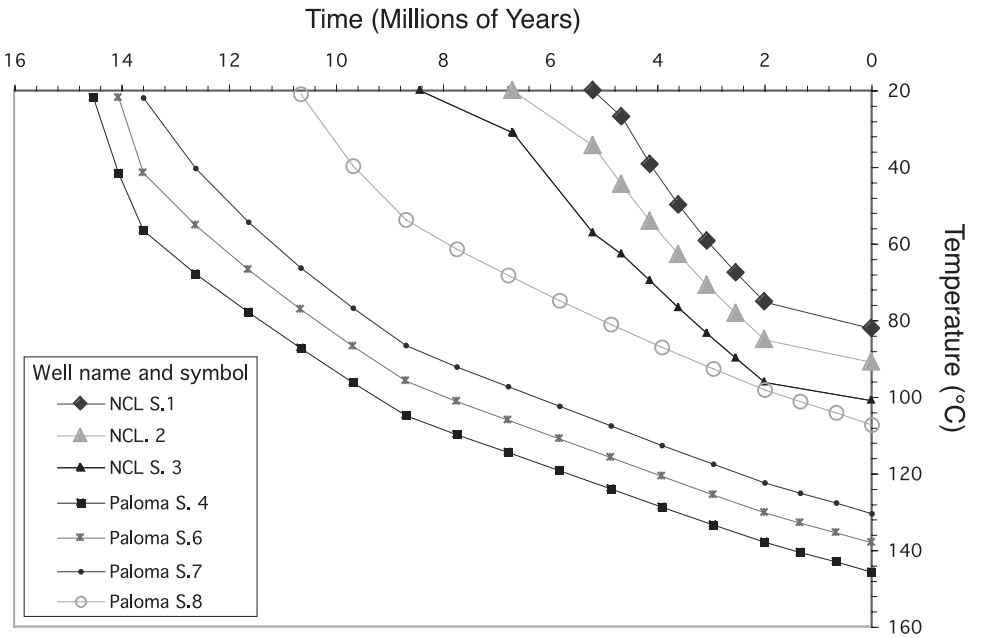

Fig. 3. Several time-temperature paths of albitized samples from the San Joaquin Basin used in the kinetic model.

MODEL FIT AND TESTS

San Joaquin Basin.—We began our search in the San Joaquin Basin. Callaway (1971) provided an excellent review of its geologic framework. In summary, the basin contains more than 7 km of Tertiary Miocene sediment, and underwent down warping by compaction during its burial history. In the center of the basin, where we focused our study, the present depths represent maximum burial. For the albitization kinetic fit, we selected from the published compositional data (Boles and Ramseyer, 1988) a total of 11 samples from nine different wells (table 4). The selection was based on the availability of thin sections and well data. We constructed time-temperature histories for each sample and determined grain sizes by averaging the diameter of 40 plagioclase grains per sample.

We extracted input parameters from the literature for basin modeling purposes, including stratigraphic information from field-scale structural cross sections (California Oil and Gas Division, 1985), formation ages (COSUNA, 1984 and Wood and Boles, 1991). The latter paper also provided formation thickness and subsidence rates. We assumed a constant basal heat flow of 50 mW/m^2, based on present day thermal data (Lachenbruch and Sass, 1980) and geothermal studies in the San Joaquin Basin (Dumitru, 1988; Wilson and others, 2000) and we used thermal conductivity values compiled in Genesis^{tm} by Zhiyong (2003). It is important to emphasize that heat fluxes in the San Joaquin Basin were likely lower than 50 mW/m^2 during active subduction, and that thermal gradients have recovered since then (Dumitru, 1988). Figure 3 depicts the resulting burial histories. The kinetic modeling search (fig. 4) indicates that the albitization trend can be reasonably simulated using an apparent activation energy of 68 $\pm$ 4 kJ/mole and apparent frequency factors of $(6.5 \pm 0.5) \times 10^3$ $1/cm^2$ Ma. The error bars in the data points (fig. 4) represent the standard deviation, computed as the square root of the variance, which is in turn calculated as the average squared deviation from the

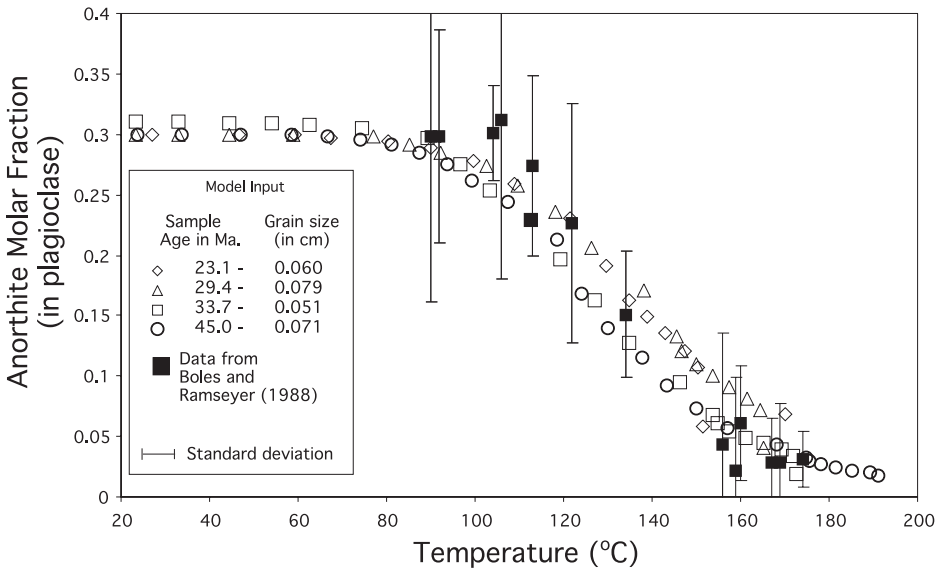

Fig. 4. Initial model fit to albitization in the San Joaquin Basin. Measured and calculated data are plotted as functions of temperature. The ■ symbol with vertical lines represents data from Boles and Ramseyer (1988) with standard deviation computed as the square root of the variance. Symbols ○, ◇, △, and □ represent sequences of simulations performed for different samples. The data fit an E_a of 68 ± 4 kJ/mol and an $A = (6.5 \pm 0.5) \times 10^3$ 1/cm^2 Ma. The E_a and A errors represent the required deviation mean value to enclose the standard deviation of the compositional data.

mean. The errors in E_a and A represents the range of values in E_a and A required to enclose the variation in the compositional data.

Tests Results

Once we calculated the set of unknown parameters in the San Joaquin Basin, we proceeded to test them against plagioclase compositional trends from the Texas Gulf Coast (Boles, 1982) and Denver Basin of Colorado (Pittman, 1988).

Texas Gulf Coast Basin.—Galloway and others (1994) provided a synthesis of the geologic, structural, and depositional history of the onshore Tertiary deposits present in the southern part of the Texas Gulf Coast Basin. The stratigraphic column in the southern part of the Texas Gulf Coast consists of 4 to 6 km of sedimentary rocks, buried in a simple down-warped fashion without major regional uplifts (Murray, 1960). Present-day depths and temperatures in the basin represent, in many cases, maximum values (Boles, 1982). We used the kinetic model and parameters derived from the San Joaquin Basin fit to simulate the plagioclase compositional trend reported for the Oligocene Frio Formation of south Texas (Boles, 1982). The data comprise eight samples distributed over eight wells from six different counties. Grain sizes were determined by measuring the mean diameter of 50 plagioclase grains in thin sections (table 4).

We constructed 1-D burial-thermal curves for each sample using Genesis^{tm} (Zhiyong, 2003). From Dodge and Posey's (1981) set of subsurface structural cross sections, we obtained well locations, formation tops, gamma-rays/spontaneous potential logs, bottom hole temperatures, and biostratigraphic information. We used the biostratigraphy information from the COSUNA (1984) chart and the U.S. Department of Interior Biostratigraphic Chart for the Gulf of Mexico (OCS) Region (2002) to derive formation ages. For the time-temperature reconstruction, the present day heat

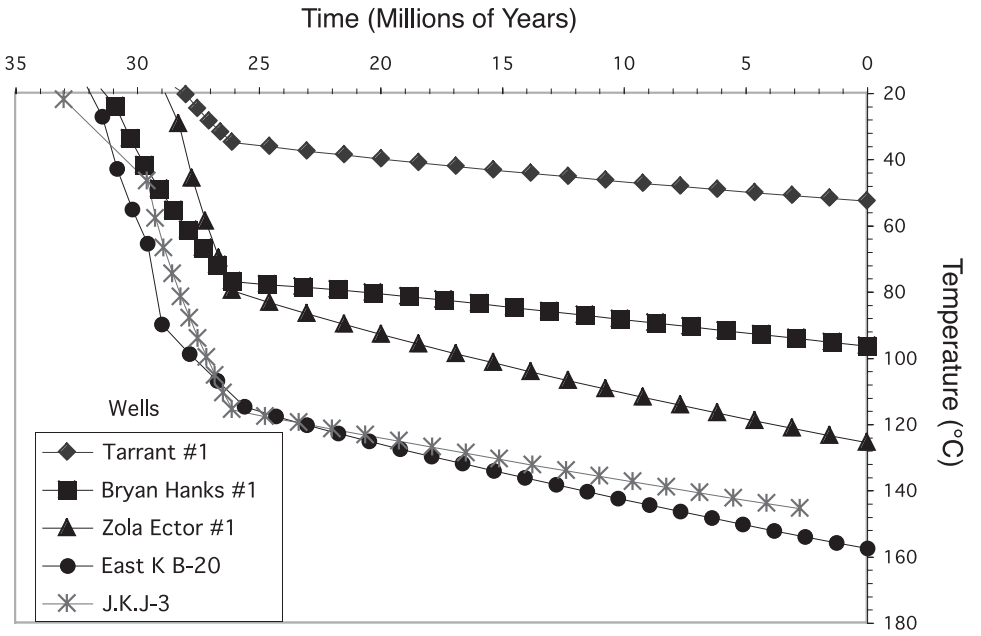

Fig. 5. Time-temperature history of albitized samples from the Gulf Coast Basin, derived from basin-burial modeling.

flux (53 mW/m^2) was set constant from the middle Oligocene to the present. The heat flux was calculated by the code using formation temperatures and thermal conductivity values compiled by Zhiyong (2003). We calibrated our time-temperature histories with temperature measurements taken along the depth of the wells (Dodge and Posey, 1981). Results are plotted in figure 5.

Using the previous results, we modeled albitization and computed the loss of the anorthite component (fig. 6A). Additionally, due to the fact that the orthoclase fraction in a detrital plagioclase remains constant and is usually less than 5 percent, an albitized grain can be conveniently studied as a binary system. In a binary system, when the compositional data is normalized to 100 percent, the variance of each component is the same, and consequently, the standard deviations are equal. Thus, we modeled the gain of the albite component using the standard deviation from the anorthite mole fraction (fig. 6B). Ten waters analysis from fluid reservoirs that have gone through different time-temperature trajectories, have significantly different ages (millions or years), and where albitization is active, the waters have relatively similar saturation index values compared to subsurface waters from the San Joaquin Basin (table 3). Thus for modeling purposes, we used the same weight averaged $\log_{10}\bar{\Omega} = 2.632$ value as in the San Joaquin Basin. The albite gain or anorthite loss during albitization in Tertiary Gulf Coast Basin can be simulated assuming reaction 2 with an apparent activation energy of 68 $\pm$ 4 kJ/mole and apparent frequency factors of (6.5 $\pm$ 0.5) $\times$ 10^3 1/cm^2 Ma. Again, errors of E_a and A represent the values required to enclose the variations in the compositional data. The error bars of the data (fig. 6B) represent the standard deviation calculated as the square root of the variance.

Denver Basin.—We tested the kinetic model against data from the Cretaceous Terry sandstone in the Spindel field, Denver Basin of Colorado. Pittman (1988 and 1989) presented a geologic synthesis of the basin and plagioclase albitization data. The history of the basin is rather complex. The heat flux varied through time resulting in

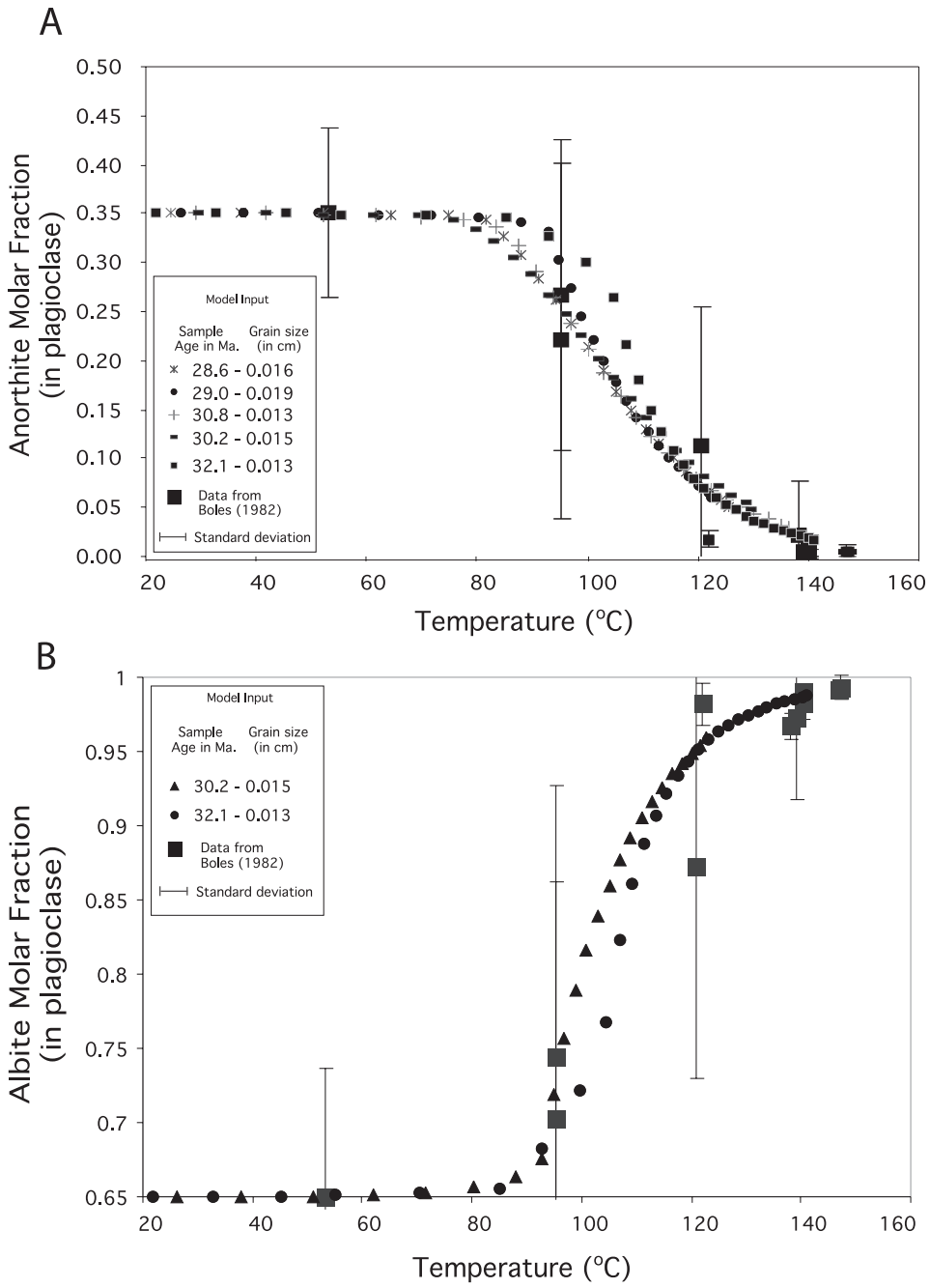

Fig. 6(A) Plot illustrating simulated and measured anorthite mole fractions versus temperature in the Gulf Coast Basin. Measured and calculated data are plotted as a function of temperature. The ■ symbol represents data extracted from Boles (1982). Vertical lines represent standard deviation of 100 spot analyses per sample, computed as the square root of the variance. All other symbols represent sequences of simulations calculated for fine-grained sandstones deposited between 28.6 and 32.1 Ma (see legend). Fit corresponds to $E_a = 68 \pm 4$ kJ/mole and $A = (6.5 \pm 0.5) \times 10^3$ 1/cm^2 Ma. The errors represent the range of values in E_a and A required to enclose the variation in the composition data.

Fig. 6(B) Calculated and measured albite mole fractions as a function of temperature in Gulf Coast Basin. The ■ symbol represents data from Boles (1982). The vertical lines represent standard deviations (square root of variance) of anorthite component. Vertical lines represent standard deviation of 100 spot analyses per sample.

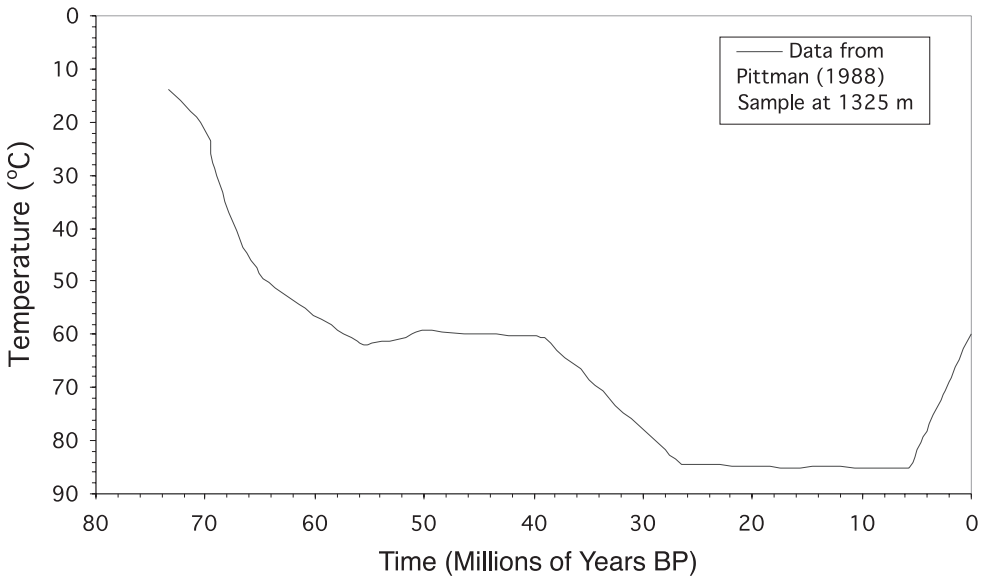

Fig. 7. Thermal history of the Terry Sandstone, Spindle field, Denver Basin, after Pittman (1988). Time-temperature profile corresponds to a horizon at ~1,325 meters depth and was used as input for albitization model.

changing thermal gradients and heating rates, and the sedimentary section was uplifted ~800 m during Early Paleocene and Miocene time. Burial and thermal histories were calibrated against R_o profiles, K/Ar data, and multiple temperature logs (Pittman, 1988).

The resulting time-temperature history of the Terry sandstone corresponds to a single horizon at ~1,325 m depth (fig. 7). Not having compositional data at specifically 1,325 m depth, we chose the closest samples where data were available, corresponding to those in the well Rademacher No. 1 at 1,283.2 and 1,286.9 m depth (see table 2, p. 752, Pittman, 1988). Albitized plagioclase in this setting was mainly reported in fine to very fine-grained sandstone. Hence, we modeled albitization using three surface area assumptions, calculated from three different sand grain sizes (1) fine grain, with d = 0.0177 cm, (2) very fine grain with d = 0.0088 cm, and (3) fine to very fine grain with d = 0.0125 cm.

Having no information regarding the oil field water chemistry or saturation indexes, we computed the reaction using the same $\log_{10}\bar{\Omega} = 2.632$ used in the San Joaquin and Gulf Coast Basin. Again, results indicate that the albitization data can be consistently predicted with an apparent activation energy of 68 ± 4 kJ/mole and apparent frequency factors of (6.5 ± 0.5) × 10^3 1/cm^2 Ma (fig. 8). The same fitting scheme performed with data from the San Joaquin Basin was performed independently using data from the Louisiana Gulf Coast and Denver Basin, and the results showed no skew.

MODEL EVALUATION

Comparison with Other Diagenetic Reactions

We compared the albitization rate constant k with the rate constants of quartz precipitation and smectite-to-illite models derived from field data and burial-temperature histories by different authors (fig. 9). Although smectite-to-illite and

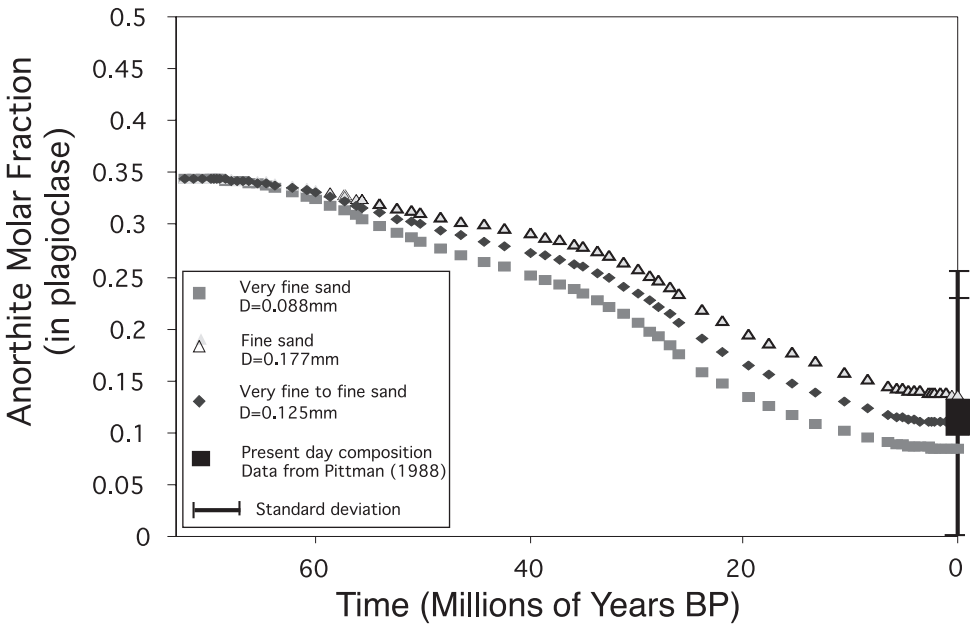

Fig. 8. Plot of comparison between calculated and measured anorthite mole fractions in Denver Basin. Measured and calculated data are plotted as a function of time. The ■ symbol represents two data points at 1,283.2 and 1,283.9 m depth (Pittman, 1988), and the error bar the standard deviation. Other symbols represent sequences of simulations performed for very fine-grained sandstones (△), fine-grained (◆) and very fine to fine sand (▣). Age of samples is ~73.3 Ma. The data fit an $E_a = 68 \pm 4$ kJ/mole and $A = (6.5 \pm 0.5) \times 10^3$ 1/cm^2 Ma. The errors in E_a and A represents the range of values in E_a and A required to enclose the variation in the composition data.

quartz precipitation are all very different reactions, their reaction rates were derived with an empirical-numerical approach, similar to ours. Additionally, smectite-to-illite and quartz overgrowth precipitation, together with albitization, constitute the main diagenetic reactions in sedimentary basins: they are all strongly dependent on heating rates and surface area or grain size. In our model, the rate constant k, is calculated with equation (32), identical to equation (4), as shown below:

$$k = Ae^{-E_a/RT} \tag{32}$$

The k is plotted in figure 9. There k ranges from $\sim 1 \times 10^{-21}$ 1/cm^2 s at 25°C to 1×10^{-18} 1/cm^2 s at 200°C (fig. 9), assuming E_a and A to be 68 kJ/mol and 6.5×10^3 1/cm^2 Ma and making the appropriate unit conversion to 1/cm^2 s.

Our rate constant values are higher than the quartz precipitation rate of Walderhaug (1994) and smectite-illite transformation rates of Huang and others (1993), and lower than Pytte and Reynolds' (1988) and Velde and Vaseur's (1992) smectite to illite rates. We also compared our model to growth rates of albite (fig. 9). Aagaard and others (1990) estimated albite growth rates from albite dissolution rates (Knauss and Wolery, 1986) and the principle of microscopic reversibility (Lasaga, 1984). According to Aagaard and others (1990), dissolution would not normally be the limiting factor in the case of K-feldspar albitization. This conclusion is reached by comparing the relatively fast K-feldspar dissolution rate (Helgeson and others, 1984) with the relatively slow albite precipitation rate—omitting nucleation.

Contrary to the K-feldspar case, in our model the rates of albitization (plagioclase dissolution) are slower than the albite growth rates of all temperatures (fig. 9), which is

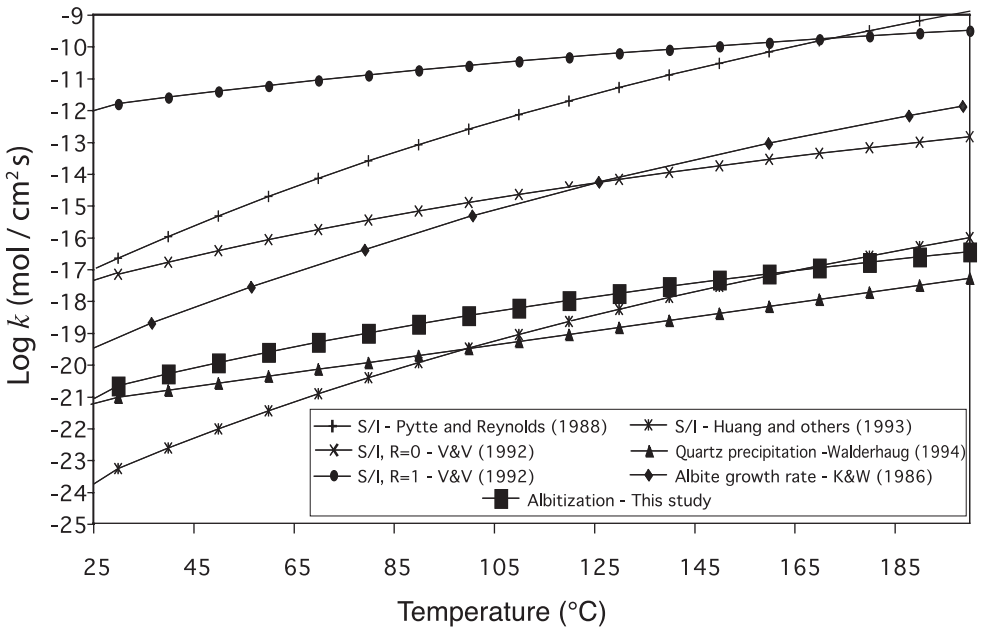

Fig. 9. Comparison of the albitization rate calculated in this paper assuming E_a 68 kJ/mole and $A = 6.5 \times 10^3$ 1/cm^2 Ma)–with other rates of mineral reactions as a function of temperature. For illitization of smectite (S/I) based on Pytte and Reynolds (1988), Velde and Vassseur (1992) and Huang and others (1993); quartz precipitation based on Walderhaug's (1994); albite growth rate based on Aagaard and others (1990).

fairly consistent with field observations. In sedimentary basins, plagioclase dissolution is the rate-limiting step of albitization based on the fact that low albite precipitates in porous sandstones at temperatures lower than the temperature onset of albitization (Ramseyer and others, 1992).

Sensitivity Studies and Model Limitations

We performed several sensitivity analyses to illustrate the model's response to variations in the input parameters. The common input to all simulations was an arbitrarily chosen time-temperature profile, somewhat similar to the thermal history of the Gulf Coast and San Joaquin Basins (fig. 10). From the simulation results (figs. 11 and 12), we are able to evaluate the effects of the initial composition and the surface area on albitization. Additionally, based on the Denver and Gulf Coast Basin results, we discuss the effect of heating rates on albitization.

Effects of initial composition.—The effect of the initial anorthite [An_0] composition on the rates of albitization is depicted in figure 11. From 0 to 65°C, the reaction rates are relatively slow and all modeled initial compositions, $An_{30}Ab_{65}$, $An_{40}Ab_{60}$, $An_{60}Ab_{30}$ and pure An_{100}, remain constant. Between 75 and 125°C all compositions are partially albitized. Finally, at temperatures over 125°C, the different compositional trends converge to a single value, that is [An] = 0 mole percent. It is clear that the plagioclase's detrital composition in terms of anorthite content affects the reaction, but the effect is minimal at high temperatures. The wide standard deviations at low temperature and small standard deviations at high temperature (figs. 4 and 6) of the data (table 1), can both be partially explained by differences in the initial anorthite fraction.

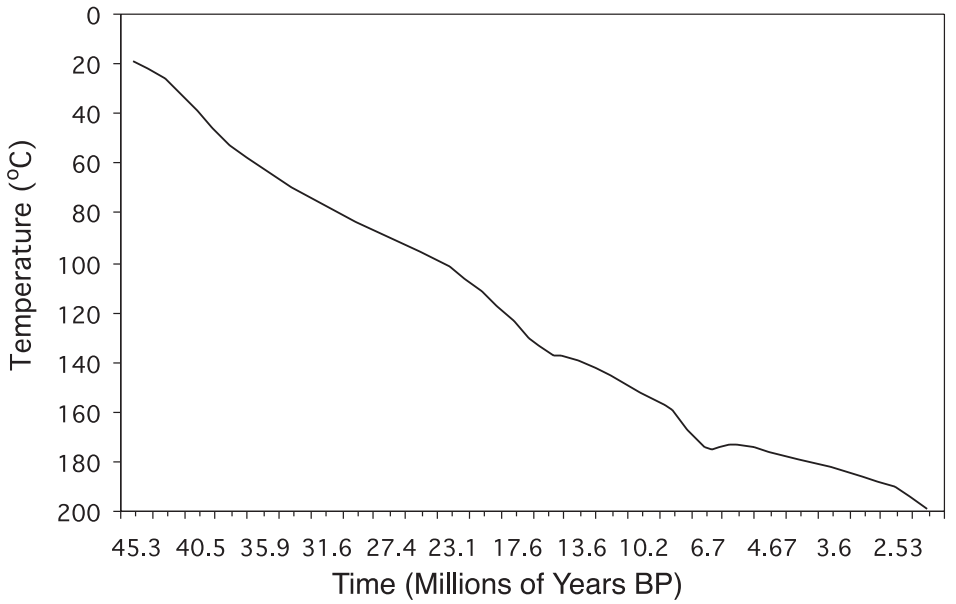

Fig. 10. Time-temperature profile representing a single burial cycle, similar to profiles from the San Joaquin and Gulf Coast Basins. This curve was used as input for several sensitivity analyses illustrated in figures 8 and 9.

Another rate determining factor to examine, but well beyond the scope of this paper, is the influence of the ordered (that is plutonic) versus disordered (that is volcanic) atomic arrangement of the albitization kinetics. At present we know of no

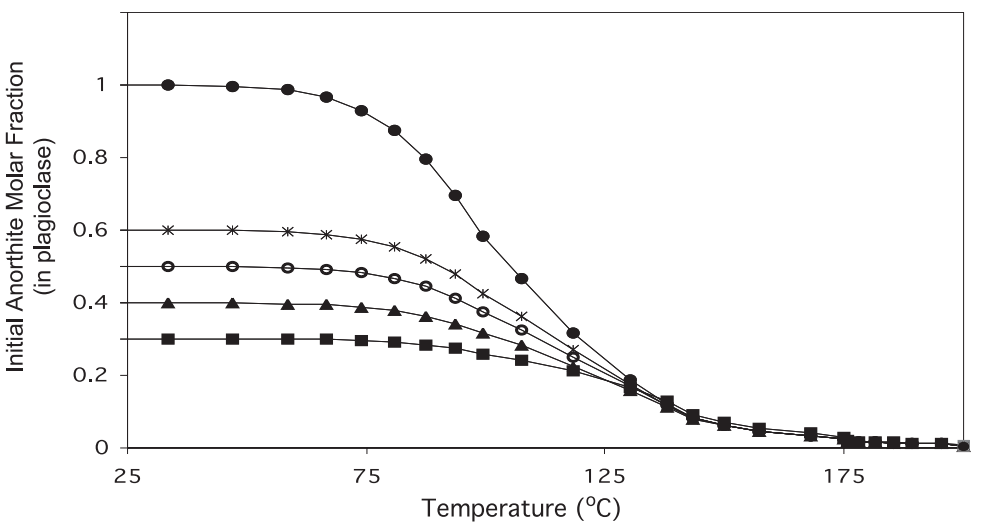

Fig. 11. Sensitivity of albitization kinetic model to plagioclase initial composition, as a function of temperature using profile in figure 7. The initial plagioclase composition is function of *An*. Simulations show that initial composition persists until ~100°C, slows albitization at temperatures below ~125°C, and converges to a single composition trend over ~135°C.

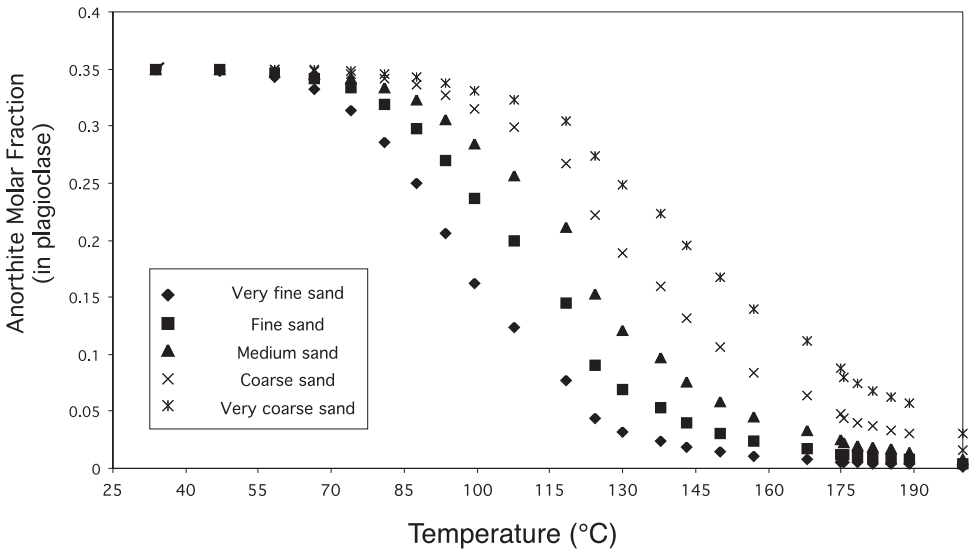

Fig. 12. Sensitivity of albitization to detrital grain size as a function of temperature. The initial plagioclase composition is common to all simulations. Simulations indicate that grain size differences affect the degree of albitization throughout the transformation. Effects of the grain size persist until high temperatures are reached, but it minimizes at temperatures over ~160°C.

thermodynamic data of ordering at constant anorthite content in plagioclase. Thus *as a proxy*, we used thermodynamic data of an hexagonal polymorph named Dmisteinbergite. This polymorph is rare but has been reported on fractured surfaces in coal from the Chelyabinsk coal basin, Southern Ural Mountains, Russia.

As mentioned the thermochemical data for hexagonal anorthite is taken from Robie and Waldbaum (1968). Hence, we calculated the equilibrium constants of reaction 2 assuming an hexagonal anorthite and graphed it in figure 2. We also calculated $\bar{\Omega}$ values for reaction 2 under the same assumption and using fluid compositions from the San Joaquin Basin and Gulf Coast Basin (table 3). The resulting values of $\log_{10}\Omega_{hexagonal}$ suggest that if Dmisteinbergite was present in the San Joaquin Basin, reaction 2 would proceed far enough to the right until the saturation point, either because the pore fluids have been in contact with sufficient amounts of the mineral or have reacted with the mineral long enough. In short, pore fluids are saturated with respect to hexagonal anorthite, and we can only speculate that the albitization of this polymorph would be faster, assuming the same rate constant.

Effect of surface area.—The mineral/fluid surface area interface is key in diagenetic modeling (Oelkers, 1996). Our model is designed such that plagioclase dissolution rate is inversely proportional to the grain diameter. A simple and direct inspection of equation (18) shows that $d[An]/dt \propto S_n$ so that $[An]_{i+1} \propto (6/d)v$. Thus, given the same initial composition and time-temperature path, smaller grains will albitize faster than bigger grains. Figure 12 illustrates albitization trends plotted against temperature for several grain diameters. Below 60°C the influence of the initial grain size on albitization is small, but over 70°C the transformation rate increases as grain size decreases. As a result plagioclase with different grain sizes may have different degrees of albitization and/or albitization paths that persist over a wide temperature range. Perhaps the wide deviations of the albitization trends may be explained by the standard deviations in grain size distributions (table 4). However, the dissolution of minerals, and particularly

feldspars, is certainly not uniform over all the surface. Leaching occurs at preferred crystallographic sites, twin planes, microfractures, and dislocations.

An additional parameter not addressed in our study is the effect of permeability on albitization. Fine-grained sandstone presumably has low initial permeability and much of its original water could be lost through compaction/cementation by the time of albitization (Boles and Coombs, 1977). Increasing albitization with increasing grain size has been reported (Boles and Coombs, 1977), but these results may indirectly reflect permeability effects rather than solely a surface area effect. Albitization requires a local steady state composition of the pore fluid, in which Ca^{+2} and Al^{+3} leave the local system on a constant rate and fluid transport is not rapid. Differences in permeability and flow rates would establish different saturation states of the fluid over short time intervals and Ω would change from one depth to another dramatically. In general, sandstone with contrasting permeability may have different anorthite content through time and different degrees of albitization.

Effect of heating rates.—Heating rates can influence the dissolution, precipitation, and even the nucleation rates of mineral reactions (Luttge and others, 1998). The effect of the heating rate on albitization can be evaluated by comparing results from our simulations. For instance the San Joaquin Basin consists of relatively young deposits, from 6.7 to 33 my, but mostly less than 20 my old, and moderate to low thermal gradients between 25 and 27°C/km. At temperatures higher than 170°C, our modeling suggest that at low temperature albite has replaced almost all plagioclase, leaving the anorthite mole fraction below 5 percent. The Gulf Coast Tertiary Basin consists of sediments 30 to 35 my old and a relatively high thermal gradient between 32 and 37°C/km. Albitization occurs there between 90 and 130°C, and at temperatures higher than 130°C the plagioclase approaches pure albite composition. In contrast, the Denver Basin was subject to periods of 50 my at temperatures in the neighborhood of 90°C, and, in our model, plagioclase has not reached pure albite composition as it does in the San Joaquin and Gulf Coast Basins. Based on these three different sets of simulations, it is clear that albitization is primarily sensitive to temperature rather than time.

The model dependence on temperature may also be evaluated by calculating time-temperature end-member values for albitization. In other words, calculating minimum temperatures at constant time (fig. 13A) and minimum times at constant temperature (fig. 13B) required to albitize plagioclase. To perform these calculations, we modeled albitization in fine-grain sandstone, set the initial composition to $An_{35}Ab_{60}Or_5$, and used our average kinetic parameters: E_a and A equal to 68 kJ/mole and 6.5×10^3 $1/cm^2$ Ma.

For the specified conditions, sedimentary rocks as old as 500 my must be subject to temperatures over 90°C in order to be albitized (fig. 10A). The minimum temperature decreases with time. Sandstone as old as 300 my must be subject to constant temperatures over 95°C, and sandstone 200 my old at temperatures over 105°C. In contrast, at temperatures over 170°C, albitization may occur in less than 0.6 my (fig. 13B).

It is important to emphasize that the replacement has a strong dependence on temperature and weak dependence on time (fig. 13). Nevertheless, these results suggest that albitization could occur slowly over long periods of time, and might occur rapidly in rocks subject to rapid thermal events, for example, thermal alteration associated with fluid flow along faults.

SOME MODEL IMPLICATIONS

With available compositional and petrologic data, our model may be used to put limits on burial and thermal histories of basins. The albitization kinetics may be used as a paleo-thermometer providing independent calibration for other thermal indicators, such as vitrinite reflectance, TAI (Thermal Alteration Index, observed by spore darkening), quartz precipitation overgrowth, and smectite-illite, in sedimentary basins.

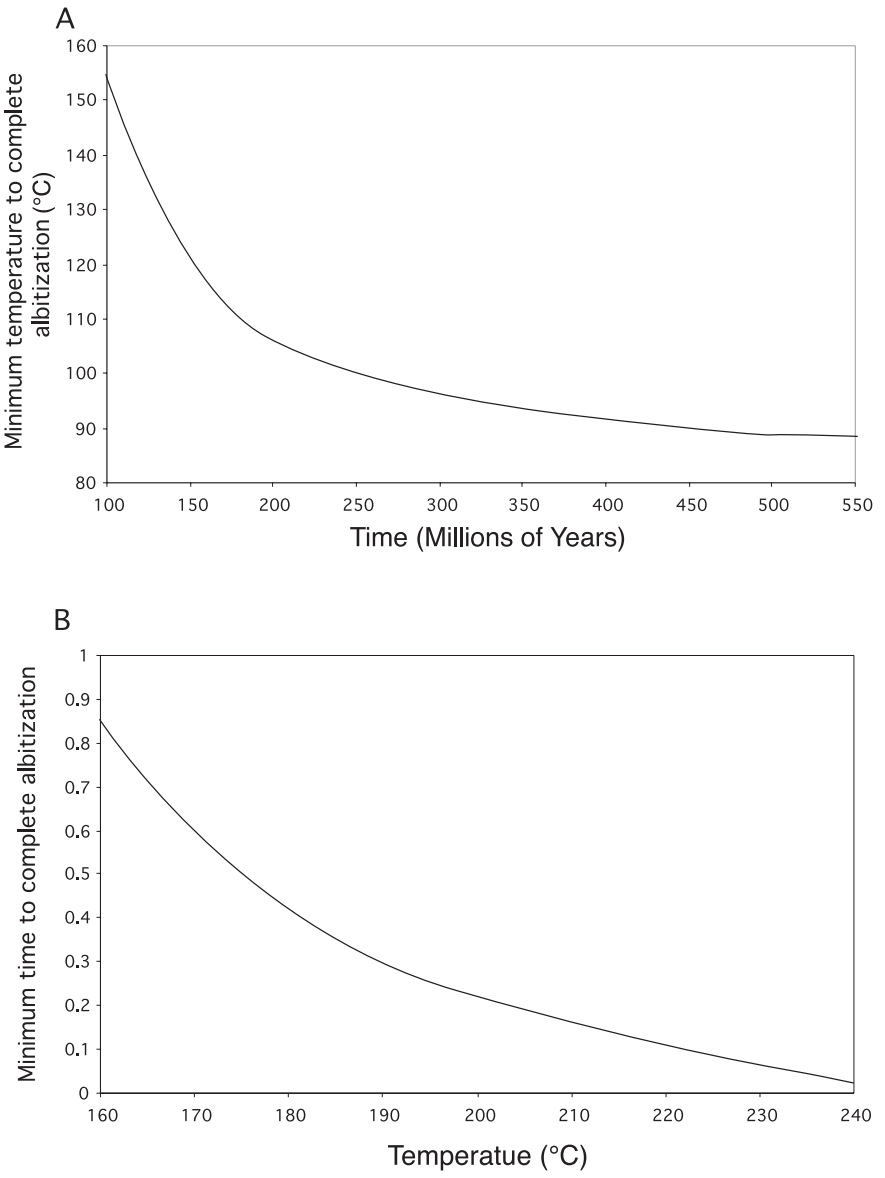

Fig. 13(A). Minimum temperatures required to complete albitization at constant time assuming fine-grained sandstone, which we considered to be an average value for all three basins. (B) Minimum time required to complete albitization at constant temperature. We assume fine-grain size sandstone, E_a = 68 kJ/mole and $A = 6.5 \times 10^3$ 1/cm^2 Ma.

The knowledge of the degree of albitization, for a given time-temperature data set, may be also useful for predicting the relative amounts of byproducts involved in reaction (2). For instance, significant Ca^{+2} enrichment in pore fluids within the albitized plagioclase zone has been reported (Fisher and Boles, 1990). The enrichment is mainly caused by the uptake of Na^+ and release of Ca^{+2} implied in reaction (2). The calcium release can now be quantitatively estimated in arkosic basins through geologic time with the albitization kinetic model. In short, the model has the potential

to lead to a better understanding of the evolution of basin fluids in geological time scales. The kinetic model may also be used by petroleum geologists for predicting the precipitation of kaolinite or calcite (assuming a CO_2 supply) associated with albitization, during burial in a given oil reservoir. Any estimation may be done by simply integrating the kinetic equation through a time-temperature burial history of a given siliciclastic formation, and applying basic rules of stoichiometry.

CONCLUSIONS

Albitization of plagioclase trends present in sedimentary basins can be reasonably reproduced with a kinetic equation that has a rate constant with a pre-exponential parameter $A = (6.5 \pm 0.5) \times 10^3$ 1/cm^2 Ma, an activation energy $E_a = 68 \pm 4$ kJ/mole and an weighted average saturation index $\log_{10}\bar{\Omega} = 2.632$. The only fitted parameter was A, the other parameters E_a and omega were fixed or calculated from real field data prior to the kinetic analysis. Our study demonstrates that time, surface area, initial composition, and primarily temperature are the most important parameters controlling the replacement reaction. Our model was tested against data from three geologic settings: Texas Gulf Coast Basin, Denver Basin of Colorado, and San Joaquin Basin with different burial and thermal histories. These results evidence that the proposed equation and its parameters can reasonably reproduce the extent of the albitization within our knowledge of variables involved.

The kinetic parameters yield rates within the range of other diagenetic reactions involving precipitation of silicates, specifically quartz overgrowth cementation, illite precipitation, and with calculations of albite crystal growth rates. The initial composition of detrital plagioclase affects albitization during the initial stages. The grain size affects albitization until the transformation is completed. Subtle differences in grain size, initial composition, and to a less extent the degree of order of the albite component may be enough to explain the wide standard deviations reported in the literature that we reference. We conclude that the albitization zone depends more on temperature and the heating rate, than time and fluid chemistry. All variables, however, are important and must be considered.

ACKNOWLEDGMENTS

We would like to acknowledge editorial work by Emma Perez and Dr. Arthur Sylvester, and constructive comments by Drs. Thomas L. Dunn and Bradley Hacker. Dr. Alicia Wilson provided important input with numerical methods and some burial histories from the San Joaquin Basin. Comments and revisions by Dr. Rolland Hellmann and the AJS anonymous reviewer greatly improved the content and theoretical basis of our study. The U.S. Department of Energy (DOE) funded our research under grant no. 444033-22433.

References Cited

1984, Correlation of Stratigraphic Units of North America (COSUNA) Project Chart, Southern California Region: Tulsa, Oklahoma, The American Association of Petroleum Geologists, chart 1.

2002, Biostratigraphic chart for the Gulf of Mexico (OCS) Region, Department of Interior-Minerals Management Service, chart 1.

Aagaard, P., and Helgeson, H. C., 1982, Thermodynamic and kinetic constraints on reaction rates among minerals and aqueous solutions, I. Theoretical considerations: American Journal of Science, v. 282, p. 237–285.

Aagaard, P., Egeberg, P. K., Saigal, G. C., Morad, S., and Bjørlykke, K., 1990, Diagenetic albitization of detrital K-feldspars in Jurassic, Lower Cretaceous and Tertiary Clastic reservoir rocks from offshore Norway, II. Formation water chemistry and kinetic considerations: Journal of Sedimentary Petrology, v. 60, p. 575–581.

Anderson, G., and Crerar, D., 1993, Thermodynamics in Geochemistry: The Equilibrium Model: New York, Oxford University Press, 588 p.

Awwiller, D. N., and Summa, L. L., 1997, Quartz cement volume constrain on burial history analysis: An example from the Eocene of Western Venezuela: American Association of Petroleum Geologists and Society of Economic Paleontologists and Mineralogists Annual Meeting, Abstracts, v. 6, p. 66.

Baccar, M. B., Fritz, B., and Made, B., 1993, Diagenetic albitization of K-feldspars and plagioclase in sandstone reservoirs: thermodynamic and kinetic modeling: Journal of Sedimentary Petrology, v. 63, p. 1100–1109.
Bailey, E. B., and Grabham, G. W., 1909, Albitization of basic plagioclase feldspars: Geological Magazine, v. 6, p. 250–256.
Bethke, C. M., 1996, Geochemical Reaction Modeling: New York, Oxford University Press, 397 p.
Blum, A. E., and Stillings, L. L., 1995, Feldspar dissolution kinetics, *in* White, A. F., and Brantley, S. L., editors, Chemical Weathering Rates of Silicate Minerals: Washington, D.C., Mineralogical Society of America Reviews in Mineralogy, v. 31, p. 291–351.
Bodart, D. E., 1980, Genetic models for the Precambrian Tarr albitite complex, southeastern Sinai: Geological Survey of Israel, p. 6–8.
Boles, J. R., 1982, Active albitization of plagioclase, Gulf Coast Tertiary: American Journal of Science, v. 282, p. 165–180.
——— 1984, Secondary porosity reactions in the Stevens sandstone, San Joaquin Valley, California, *in* McDonald, D. A., and Surdam, R. C., editors, Clastic Diagenesis: AAPG Memoir 37, p. 217–224.
Boles, J. R., and Coombs, D. S., 1977, Zeolite facies alteration of sandstones in the Southland syncline, New Zealand: American Journal of Science, v. 277, p. 982–1012.
Boles, J. R., and Franks, S. G., 1979, Clay diagenesis in Wilcox sandstones of southwest Texas: implications of smectite diagenesis on sandstone cementation: Journal of Sedimentary Petrology, v. 49, p. 55–70.
Boles, J. R., and Ramseyer, K., 1988, Albitization of plagioclase and vitrinite reflectance as paleothermal indicators, San Joaquin Basin, *in* Graham, S. A., editor, Studies in the Geology of the San Joaquin Basin: Pacific Section and Society of Economic Paleontologists and Mineralogists, v. 60, p. 129–139.
Burnham, A. K., and Sweeney, J. J., 1989, A chemical kinetic model of vitrinite maturation and reflectance: Geochimica et Cosmochimica Acta, v. 53, p. 2649–2657.
Burnham, A. K., Braun, R. L., Greg, H. R., and Samoun, A. M., 1987, Comparison of methods for measuring kerogen pyrolisis rates and fitting kinetic parameters: Energy and Fuels, v. 1, p. 452–458.
California Oil and Gas Fields, 1985, Central California: California Department of Conservation Division of Oil and Gas, 3rd edition, 1000 p.
Callaway, D. C., 1971, Petroleum potential of the San Joaquin Basin, California, *in* Cram, I. H., editor, Future Petroleum Provinces of the United States-Their geology and potential: American Association of Petroleum Geologists Memoir 15, p. 239–253.
Comer, J., 1992, Thermal Alteration, *in* Pratt, L., Comer, J., and Brassell, S., editors, Geochemistry of Organic Matter in Sediments and Sedimentary Rocks: SEPM Short Course 27: Tulsa, Oklahoma, Society for Sedimentary Geology, p. 73–100.
Coombs, D. S., 1954, The nature and alteration of some Triassic sediments from Southland, New Zealand: Royal Society New Zealand Transactions, v. 82, p. 65–109.
Davisson, M. L., and Criss, R. E., 1996, Na-Ca-Cl relations in basinal fluids: Geochimica et Cosmochimica Acta, v. 60, p. 2743–2752.
Deer, W. A., Howie, R. A., and Zussman, J., 1963, Framework silicates: Rock-forming minerals, v. 4: London, Longmans, 435 p.
Dewers, T., and Ortoleva, P., 1990, Force of crystallization during the growth of siliceous concretions: Geology, v. 18, p. 204–207.
Dodge, M. M., and Posey, J. S., 1981, Structural cross sections, Tertiary formations, Texas Gulf Coast: Austin, The University of Texas Austin, 6 p.
Dumitru, T. A., 1988, Subnormal geothermal gradients in the Great Valley forearc basin, California, during Franciscan subduction; a fission track study: Tectonics, v. 7, p. 1201–1221.
Elliot, C. W., and Matisoff, G., 1996, Evaluation of kinetic models for the smectite to illite transformation: Clays and Clay Minerals, v. 44, p. 77–87.
Eskola, P., Vuoristo, U., and Rankama, K., 1935, An experimental illustration of spilite reaction: Comptes Rendus de la Society geologique de Finlande.
Fisher, J. B., and Boles, J. R., 1990, Water-rock interaction in Tertiary sandstones, San Joaquin Basin, California, U.S.A.: Diagenetic controls on water composition: Chemical Geology, v. 83, p. 83–101.
Fox, L. K., ms, 1989, Albitization of Jurassic plutons in the southern Bristol Mountains, east-central Mojave Desert, southeastern California: Ph. D. thesis, University of California, Santa Barbara, 324 p.
Gallagher, K., and Evans, E., 1991, Estimating kinetic parameters for organic reactions from geological data: an example from the Gippsland basin, Australia: Applied Geochemistry, v. 6, p. 653–664.
Galloway, W. E., Liu, K., Travis-Neuberger, D., and Xue, L., 1994, Reference high-resolution correlation, cross sections, Paleogene section, Texas, Coastal plain: Austin, The University of Texas at Austin, 19 p.
Garven, G., 1995, Continental-scale groundwater flow and geological processes: Annual Review of Earth and Planetary Sciences, v. 23, p. 89–117.
Gold, P. B., 1987, Textures and geochemistry of authigenic albite from Miocene sandstones, Louisiana Gulf Coast: Journal of Sedimentary Petrology, v. 57, p. 353–362.
Hayes, M. J., and Boles, J. R., 1992, Volumetric relations between dissolved plagioclase and kaolinite in sandstones: Implications for aluminum mass transfer in the San Joaquin Basin, California, *in* Houseknecht, D. W., and Pittman, E. D., editors, Origin, Diagenesis, and Petrophysics of Clay Minerals in Sandstones: Tulsa, Oklahoma, SEPM Special Publication, No. 47, p. 111–123.
Helgeson, H. C., Murphy, W. M., and Aagaard, P., 1984, Thermodynamic and kinetic constraints on reaction rates among minerals and aqueous solutions. II. Rate constants, effective surface area, and the hydrolysis of feldspar: Geochimica et Cosmochimica Acta, v. 48, p. 2405–2432.
Helgeson, H. C., Knox, A. m., Owens, C. E., and Shock, E. L., 1993, Petroleum, oil field waters, and authigenic mineral assemblages: Are they in metastable equilibrium in hydrocarbon reservoirs?: Geochimica et Cosmochimica Acta, v. 57, p. 3295–3339.

Hellmann, R., 1994, The albite-water system: Part I. The kinetics of dissolution as a function of pH at 100, 200 and 300 C: Geochimica et Cosmochimica Acta, v. 58, p. 595–611.
Hess, H. H., 1950, Vertical mineral variation in the Great Dyke of Southern Rhodesia: Transactions Geological Society South Africa, v. 53, p. 159.
Huang, W., Longo, J., and Pevear, D., 1993, An experimentally derived kinetic model for smectite-to-illite conversion and its use as a geothermometer: Clays and Clay Minerals, v. 41, p. 162–177.
Johnson, J. W., Oelkers, E. H., and Helgeson, H. C., 1992, SUPCRT92: A software package for calculating the standard molal thermodynamic properties of minerals, gases, aqueous species, and reactions from 1 to 5000 bar and 0 to 1000 C: Computers and Geosciences, v. 18, p. 899–947.
Kharaka, Y. K., and Barnes, J. A., 1973, SOLMINEQ: solution-mineral equilibrium computations: U.S. Geological Survey Computer Contributions Report, p. 215–899.
Knauss, K. G., and Wolery, T. J., 1986, Dependence of albite solution kinetics on pH and time at 25 C and 70 C: Geochimica et Cosmochimica Acta, v. 50, p. 2481–2497.
Labotka, T., Cole, D., Mostafa, F., and Riciputi, L., 2002, Coupled cation and oxygen exchange between alkali feldspar and aqueous chloride solution: Goechimica et Cosmochimica Acta, v. 66, p. A427.
Lachenbruch, A. H., and Sass, J. H., 1980, Heat flow and energetics of the San Andreas fault zone: Journal of Geophysical Research, v. 85, p. 6185–6222.
Land, L. S., and Milliken, K. L., 1981, Feldespar diagenesis in the Frio Formation, Brazoria County, Texas Gulf Coast: Geology, v. 9, p. 314–318.
Lander, R., and Walderhaug, O., 1999, Predicting porosity through simulating sandstone compaction and quartz cement: American Association of Petroleum Geologists Bulletin, v. 83, p. 433–449.
Lasaga, A., 1984, Chemical kinetics of water-rocks interactions: Journal of Geophysical Research, v. 89, p. 4009–4025.
——— 1995, Fundamental approaches in describing mineral dissolution and precipitation rates, *in* White, A. F., and Brantley, S. L., editors, Chemical Weathering Rates of Silicate Minerals: Washington, D.C., Mineralogical Society of America, Reviews in Mineralogy and Geochemistry, v. 31, p. 23–86.
——— 1998, Kinetic theory in the earth sciences: Princeton, Princeton University Press, 811 p.
Lopatin, N. V., 1971, Temperature and geological time as factors of carbonifaction: Akademiya Nauk SSSR Izvestiya, Seriya Geologicheskaya, v. 3, p. 95–106.
Luttge, A., and Metz, P., 1991, Mechanism and kinetics of the reaction: 1 dolomite + 2 quartz = 1 diopside + 2 CO_2 investigated by powder experiments: Canadian Mineralogist, v. 4, p. 803–821.
——— 1993, Mechanisms and kinetics of the reaction: 1 dolomite + 2 quartz = 1 diopside + 2 CO_2. A comparison of rock-sample and powder experiments: Contributions to Mineralogy and Petrology, v. 115, p. 155–164.
Luttge, A., Neumann, U., and Lasaga, A., 1998, The influence of heating rate on the kinetics of mineral reactions: An experimental study and computer models: American Mineralogist, v. 83, p. 501–515.
Mackenzie, A. S., and Mackenzie, D. P., 1983, Isomerization and aromatization of hydrocarbons in sedimentary basins formed by extension: Geological Magazine, v. 220, p. 417–470.
Maliva, R. G., and Siever, R., 1988, Diagenetic replacement controlled by force of crystallization: Geology, v. 96, p. 688–691.
Matthews, A., 1980, Influences of kinetics and mechanism in metamorphism: a study of albite crystallization: Geochimica et Cosmochimica Acta, v. 44, p. 387–402.
Merino, E., 1975a, Diagenesis in Tertiary sandstones from Kettleman North Dome, California - II. Interstitial solutions: distribution of aqueous species at 100 C and chemical relation to the diagenetic mineralogy: Geochimica et Cosmochimica Acta, v. 39, p. 1629–1645.
——— 1975b, Diagenesis in Tertiary sandstones from Kettleman North Dome, California: I. Diagenetic mineralogy: Journal of Sedimentary Petrology, v. 45, p. 320–336.
Merino, E., and Dewers, T., 1998 Implications of replacement for reaction-transport modeling. Journal of Hydrology, v. 209, p. 137–146.
Merino, E., Nahon, D., and Yifeng, W., 1993, Kinetics and mass transfer of pseudomorphic replacement: application to replacement of parent minerals and kaolinite by Al, Fe, and Mn oxides during weathering: American Journal of Science, v. 293, p. 135–155.
Middleton, G., 1972, Albite of secondary origin in Charny Sandstones, Quebec: Journal of Sedimentary Petrology, v. 42, p. 341–349.
Moody, J. B., Jenkins, J. E., and Meyer, D., 1985, An experimental investigation of the albitization of plagioclase: Canadian Mineralogist, v. 23, p. 583–592.
Morad, S., Morten, B., Knarud, R., and Nystuen, J., 1990, Albitization of detrital plagioclase in Triassic reservoir sandstones from the Snorre Field, Norwegian North Sea: Journal of Sedimentary Petrology, v. 60, p. 411–425.
Murray, G. E., 1960, Geological framework of Gulf Coastal Province of United States, *in* Shepard, F. P. a. o., editor, Recent sediments, northwestern Gulf of Mexico: Tulsa, Oklahoma, American Association of Petroleum Geologists Publication, p. 5–33.
Nahon, D., and Merino, E., 1997, Pseudomorphic replacement in tropical weathering: evidence, geochemical consequences, and kinetic-rheological origin: American Journal of Science, v. 297, p. 393–417.
Oelkers, E. H., 1996, Physical and Chemical Properties of Rock and fluids for chemical mass transport calcultations, *in* Litchtner, P. C., Steefel, C. I., and Oelkers, E. H., editors, Reactive Transport in Porous Media: Reviews in Mineralogy, Mineralogical Society of America, v. 34, p. 131–182.
Oelkers, E. H., Bjorkum, P. A., and Murphy, W. M., 1996, A petrographic and computational investigation of quartz cementation porosity reduction in North Sea sandstones: American Journal of Science, v. 296, p. 420–452.

Oelkers, E. H., Bjorkum, P. A., Walderhaug, O., Nadeau, P. H., and Murphy, W. M., 2000, Making diagenesis obey thermodynamics and kinetics: the case of quartz cementation in sandstones from offshore mid-Norway: Applied Geochemistry, v. 15, p. 295–309.

O'Neil, J. R., 1977, Stable isotopes in Mineralogy: Physics and Chemistry of Minerals, v. 2, p. 105–123.

O'Neil, J. R., and Taylor, H. P., Jr., 1967, The oxygen isotope and cation exchange chemistry of feldspars: American Mineralogist, v. 52, p. 1414–1437.

Perez, R. J., Chatellier, J. Y., and Lander, R. H., 1999a, Use of quartz cementation kinetic modeling to constrain burial histories. Examples from the Maracaibo basin, Venezuela: Revista Latinoamericana de Geoquimica Organica, v. 5, p. 39–46.

Perez, R. J., Gosh, S., Chatellier, J. Y., and Lander, R. H., 1999b, Application of sandstone diagenetic modeling to reservoir quality assessment of the Misoa Formation, Bachaquero Field, Maracaibo Basin, Venezuela: Annual Meeting Expanded Abstracts - American Association of Petroleum Geologists, v. 1999, p. A107.

Perkins, E. H., Kharaka, Y. K., Gunter, W. D., and DeBraal, J. D., 1990, Geochemical modeling of water-rock interactions using SOLMINEQ.88, *in* MELCHIOR, D. C., and BASSETT, R. L., editors, Chemical Modeling of Aqueous Systems II: American Chemical Society Symposium Series: Washington, D.C., American Chemical Society, p. 117–127.

Pittman, E. D., 1988, Diagenesis of Terry sandstone (Upper Cretaceous), Spindle Field, Colorado: Journal of Sedimentary Petrology, v. 58, p. 785–800.

——— 1989, Nature of the Terry sandstone Reservoir, Spindle Field, Colorado, *in* Coalson, E. B., Editor, Sandstone Reservoirs: Denver, The Rocky Mountain Association of Geologists, p. 245–254.

Putnis, A., 2002, Mineral replacement reactions: from macroscopic observations to microscopic mechanisms: Mineralogical Magazine, v. 66(5), p. 689–708.

Pytte, A., and Reynolds, R., 1988, The thermal transformation of smectite to illite, *in* Nasser, N., and McCulloh, T., editors, Thermal history of sedimentary basins: Berlin, Springer-Verlag, p. 133–140.

Ramseyer, K., Boles, J. R., and Lichtner, P. C., 1992, Mechanisms of Plagioclase Albitization: Journal of Sedimentary Petrology, v. 62, p. 349–356.

Reyhani, M. M., Freij, S., and Parkinson, G. M., 1999, *In situ* atomic force microscope investigation of the growth of secondary nuclei produced by contact of different growth phases of potash alum crystals under supersaturated solutions: Journal of Crystal Growth, v. 198/99, p. 258–263.

Robie, R. A., and Waldbaum, D. R., 1968, Thermodynamic properties of minerals and related substances at 298.15 K (25 C) and one atmosphere (1.1013 bars) pressure and at higher temperatures: Geological Survey Bulletin, v. 1259, p. 1–256.

Rosenbauer, R. J., Bishoff, J. L., and Zierenberg, R. A., 1988, The laboratory albitization of mid-ocean ridge basalt: Journal of Geology, v. 96, p. 237–244.

Saxena, S. K., and Ribbe, P. H., 1972, Activity-composition relations in feldspars: Contributions to Mineralogy and Petrology, v. 37, p. 131–138.

Siever, R., 1983, Burial history and diagenetic reaction kinetics: American Association of Petroleum Geologist, Bulletin, v. 67, n. 4, p. 684–6911.

Slaby, E., 1992, Changes in the structural state of secondary albite during progressive albitization: Neues Jahbruch fuer Mineralogie, Monatshefte, v. 7, p. 321–335.

Smith, J. V., 1972, Critical review of synthesis and occurrence of plagioclase feldspars and possible phase diagram: Journal of Geology, v. 80, p. 505–525.

Stallard, M. L., and Boles, J. R., 1989, Oxygen isotope measurements of albite-quartz-zeolite mineral assemblages, Hokonui Hills, Southland, New Zealand: Clay and Clay Minerals, v. 37, p. 409–418.

Tester, A. C., and Atwater, G. I., 1934, The occurrence of authigenic feldspar in sediments: Journal of Sedimentary Petrology, v. 4, p. 23–31.

Velde, B., and Vasseur, G., 1992, Estimation of the diagenetic smectite to illite transformation in time-temperature space: American Mineralogist, v. 77, p. 967–976.

Walderhaug, O., 1994, Precipitation rates for quartz cement in sandstones determined by fluid-inclusion microthermometry and temperature-history modeling: Journal of Sedimentary Research, v. A64, p. 324–333.

——— 1996, Kinetic modeling of quartz cementation and porosity loss in deeply buried sandstone reservoirs: American Association of Petroleum Geologists Bulletin, v. 80, p. 731–745.

Walther, J. V., and Wood, B. J., 1984, Rate and mechanism in prograde metamorphism: Contributions to Mineralogy and Petrology, v. 88, p. 246–259.

Waples, D. W., 1980, Time and temperature in petroleum formation: Application of Lopatin's method to petroleum exploration: American Association of Petroleum Geologist Bulletin, v. 64, p. 916–926.

Wilson, A., Boles, J., and Garven, G., 2000, Calcium mass transport and sandstone diagenesis during compaction-driven flow: Stevens Sandstone, San Joaquin Basin, California: Geological Society of America Bulletin, v. 112, p. 845–856.

Winkler, U., and Luttge, A., 1999, The influence of $CaCl_2$ on the kinetics of the reaction 1Tremolite + 3Calcite + 2Quartz = 5Diopside + $3CO_2$ +$1H_2O$. An experimental investigation: American Journal of Science, v. 299, p. 393–427.

Wood, J. R., and Boles, J. R., 1991, Evidence for episodic cementation and diagenetic recording of seismic pumping events, North Coles Levee, California, U.S.A.: Applied Geochemistry, v. 6, p. 509–521.

Zhiyong, H., 2003, "Theoretical and numerical basis for Genesis 1D basin modeling": Downloaded January 28, http://www.zetaware.com/.